A Publication for the
Radio Amateur Worldwide

Especially Covering VHF,
UHF and Microwaves

VHF COMMUNICATIONS

Volume No. 24 . Spring . 1/1992 . £3.50

DB1NV:
Tracking Generator for the Spectrum Analyser

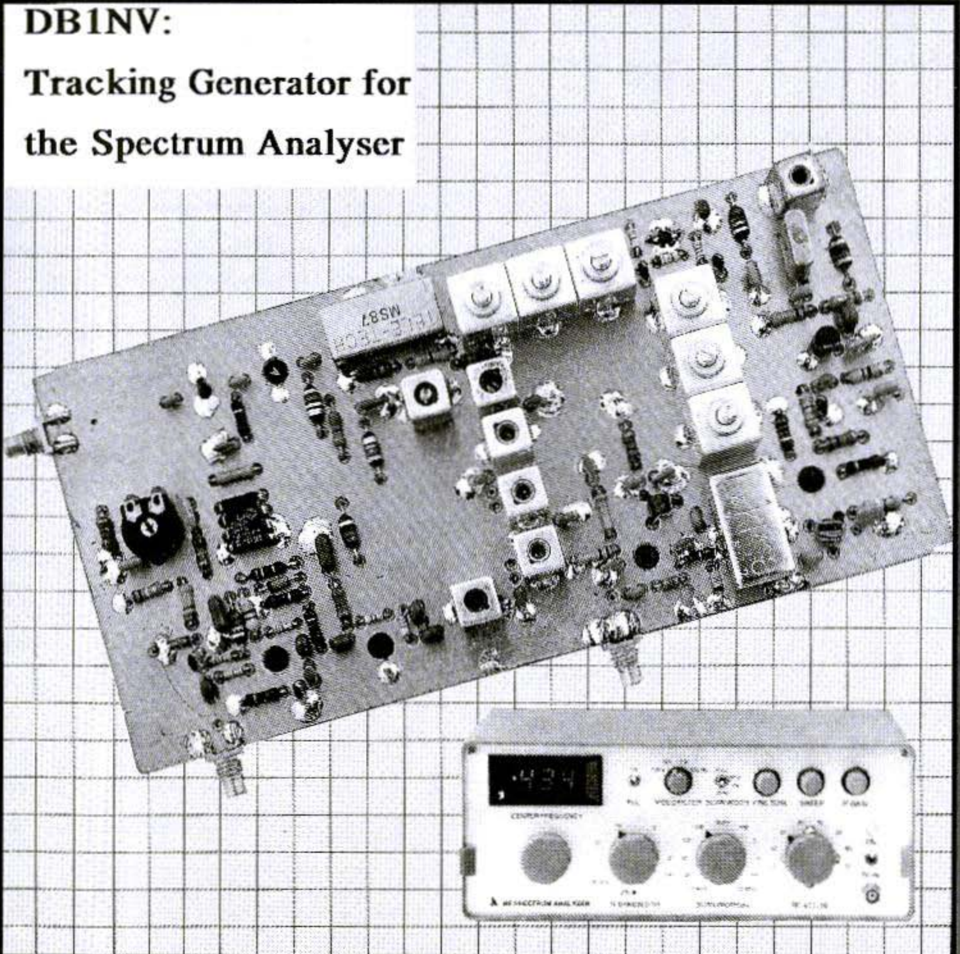

VHF COMMUNICATIONS

A Publication for the Radio Amateur Worldwide

Especially Covering VHF, UHF and Microwaves

Volume No. 24 . Spring . Edition 1/1992

Published by: KM PUBLICATIONS, 5 Ware Orchard, Barby, Nr. Rugby, CV23 8UF, United Kingdom.

Publishers: KM PUBLICATIONS

Editors: Mike Wooding G6IQM, Kim Wooding

Advertising Manager: Mike Wooding G6IQM

VHF COMMUNICATIONS

The international edition of the German publication UKW-BERICHTE is a quarterly amateur radio magazine especially catering for the VHF/UHF/SHF technology. It is published in Spring, Summer, Autumn and Winter under licence in the United Kingdom by KM PUBLICATIONS.

The 1992 subscription price is £12.00, or national equivalent per year. Individual copies are available at £3.50, or national equivalent each. Subscriptions, orders of individual copies, advertisements and contributions to the magazine should be addressed to the national representative, or - if not possible - directly to the publishers.

Back copies, kits, as well as the blue plastic binders are obtainable from your national representative or from KM Publications in the U.K.

Translated by Inter-Ling Services Ltd., 30-32 Regent Place, Rugby, Warwickshire, CV21 2PN, U.K.

Printed in the United Kingdom by: Apex Printers, 1 Avon Industrial Estate, Butlers Leap, Rugby, CV21 3UY.

Please address your orders or enquiries to your representative.

REPRESENTATIVES:

A U S T R I A - Verlag UKW-BERICHTE, Terry D. Bittan, POB 80, D-8523 Baiersdorf, West Germany. Telephone: (9133) 47-0. Telex: 629 887. Postgiro Nbg: 30455-858. Fax: 09733 4747.

A U S T R A L I A - W.I.A., P.O. Box 300, South Caulfield, 3162 VIC, Australia. Telephone: 5285962.

B E L G I U M - UKW.Berichte, P.O. Box 80, D-8523 Baiersdorf, West Germany. Tel: 09133-47-0. Postgiro: Nbg. 30455-858. Fax: 09133-4747.

D E N M A R K - HALSKOV ELECTRONIC OZ7LX, Sigersted gamle Skole, DK-4100 RINGSTED, Denmark. Telephone: 53-616162 (kl.19-22). Giro: 7 29 68 00.

F R A N C E - Christianne Michèl F5SM, SM ELECTRONIC, 20 bis, Avenue des Clarions, F-89000 AUXERRE, France. Telephone: (86) 46 96 59.

F I N L A N D - Peter Lytz OH2AVP, Yläkartanonkuja 5 A 9, SF-02360 ESPOO, Finland.

SRAT, PL 44, SF-00441 HELSINKI, Finland. Telephone: 358/0/5625973.

G E R M A N Y - UKW.Berichte, P.O. Box 80, D-8523 Baiersdorf, West Germany. Tel: 09133-47-0. Postgiro: Nbg. 30455-858. Fax: 09133-4747.

G R E E C E - C+A ELECTRONIC, P.O. Box 25070, Athens 100 26, Greece. Telephone: 01 52 42 867. Fax: 01 52 42 537

H O L L A N D - KM PUBLICATIONS, 5 Ware Orchard, Barby, Nr. Rugby, CV23 8UF, U.K. Telephone: 0788 890365.

I S R A E L - Doron Jacobi 4Z4RG, P.O. Box 6382, HAIFA, Israel 31063.

I T A L Y - ADB ELETTRONICA di Lucchesi Fabrizio IW5ADB, Via del Cantone 714, 55100 ANTRACCOLI (LUCCA), Italy. Telephone: 0583-952612.

L U X E M B O U R G - TELECO, Jos. Faber LX1DE, 5-9 Rue de la Fontaine, ESCH-SUR-ALZETTE, Luxembourg.

N E W Z E A L A N D - E.M.Zimmerman ZL1AGQ, P.O.Box 31-261, Milford, AUCKLAND 9, New Zealand. Telephone: (9) 486 2744.

N O R W A Y - HENNING THEG RADIO COMMUNICATION LA4YG, Kjøinveien 30, 1370, ASKER, Norway. Postgirokonto: 3 16 00 09.

S O U T H A F R I C A - HI-TECH BOOKS, P.O.Box 1142, RANDBURG, Transvaal 2125, South Africa. Telephone: (011) 886-2020.

S P A I N & P O R T U G A L - Julio A. Prieto Alonso EA4CJ, MADRID-15, Donoso Cortès 58 5"-B, Spain. Telephone: 543.83.84.

S W E D E N - Lars Pettersson SM4IVE, Pl. 1254, Smégården Talby, S-17500 ODENSBACKEN, Sweden. Telephone: 19-50223. Postgiro: 914379-3.

S W I T Z E R L A N D - Terry Bittan. PSchKto. ZÜRICH 80-54.849-8.

U N I T E D K I N G D O M - KM PUBLICATIONS, 5 Ware Orchard, Barby, Nr. Rugby, CV23 8UF. Telephone: 0788 890365 & 0788 561281. FAX: 0788 890365

U S A - WYMAN RESEARCH INC., RR#1 Box 95, Waldron, Indiana 46182, USA. Telephone: (317) 525-6452.
HENRY RUH, ATVQ MAGAZINE, 1545 Lee Street, Suite 73, Des Plaines, IL. 60018, USA. Tel: (708) 298 2269. FAX: (708) 291 1644.

ISSN 0177-7505

Contents

KM Publications, 5 Ware Orchard, Barby, Nr. Rugby, CV23 8UF, U.K.

Telephone: U.K: 0788 890365; INT: + 44 788 890365. FAX: 0788 890365

Rainer Tappert, 8261 Oberberglirchen

ATV with twin Sound Channels Part-2 (conclusion)

3.4.1 The Intercarrier Receiver

The intercarrier system has the advantage of simple signal handling at IF level and requires the lowest expenditure (Fig.7). This cost-effective solution is at the cost of objectionable intercarrier buzz, which consists mainly of field and line frequency and of components of the line frequency. In addition, titles keyed in electronically can cause interference on sound.

3.4.2 Parallel Sound System

In the technically best variant, the parallel sound technique, the intercarrier interference is avoided. Circuit-wise, the sound is not regenerated by taking the difference between the sound and vision carriers, but instead each channel has its own IF amplifier (audio 1 = 33.4MHz, audio 2 = 33.15MHz), as Fig.8 indicates. Currently the parallel sound system is employed only in very high quality (expensive) receivers.

3.4.3 Quasi-Parallel Sound System

An interesting variant is the so-called quasi-parallel sound receiver. It avoids the interference from keyed-in text but exhibits all the other disadvantages of intercarrier receivers.

Parallel denotes the parallel signal processing following the tuner, quasi is in relation to the intercarrier system (Fig.9). In comparison to the system described in 3.4.1 it is visible that due to the separation of the two signal paths, each stage can be optimised as appropriate.

4. ENHANCEMENTS TO THE TRANSMITTER

4.1 Modulator and Automatic Frequency Control

Anyone expecting a circuit diagram and constructional advice at this stage is going to be disappointed, since as was already indica-

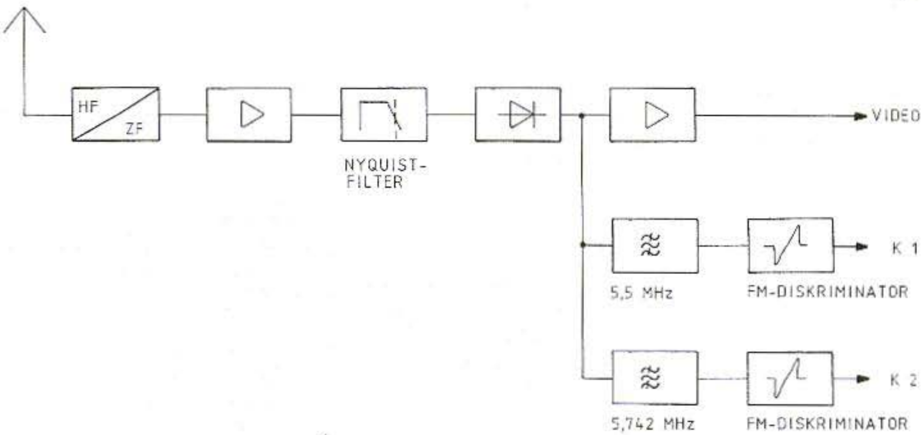

Fig.7: Signal Route in the Intercarrier System

ted in section 3.2 and shown in the block diagram (Fig.5), the second sound channel uses the DJ4LB 002 module from VHF COMMUNICATIONS 1/1972. Everything mentioned there is still valid for this enhancement. Alignment is, however, not at 33.4MHz but at 33.15MHz. Also the AFC (automatic frequency control) can be adopted without alterations (DJ6PI 003).

The internally generated comparison frequency is, in contrast with the original description, aligned using L3 to 5.742MHz, also the input circuit.

Incidentally, the precise alignment of the frequency comparison stage is described in VHF COMMUNICATIONS German issue 4/1975 and can be read up there.

4.2 The Diplexer

The uncritical circuit in Fig.10 was built on a trial basis on Veroboard and worked fault-free the first time round. All the same a tinplate screening case of the appropriate dimensions must not be forgotten; the inputs and outputs can be brought through conveniently using BNC flange sockets.

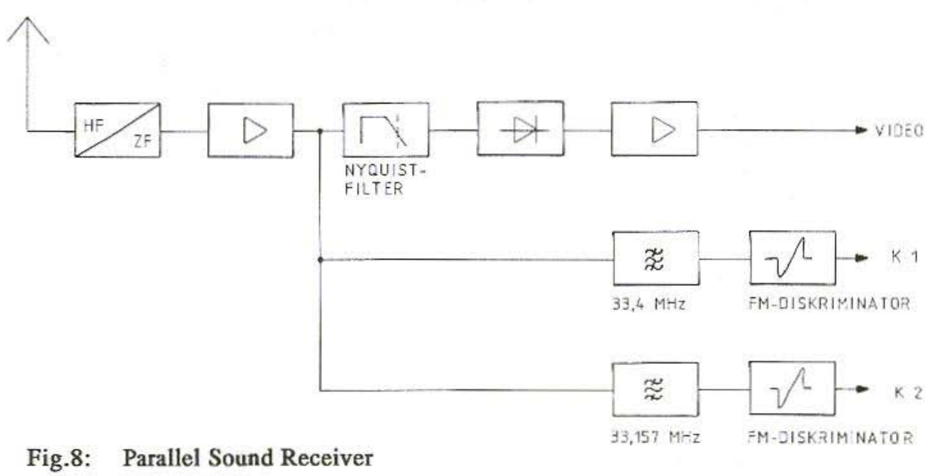

Fig.8: Parallel Sound Receiver

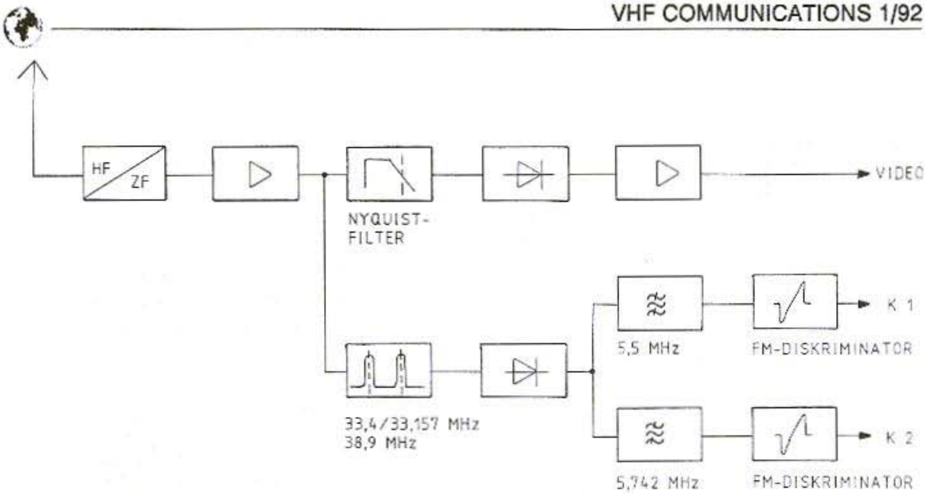

Fig.9: Intercarrier Receiver (Quasi-Parellel Sound System)

The transistor BF191 works in collector mode. The two sound IF inputs are fed together via a resistor network and matched. The two potentiometers P1 and P2 allow the level of the two sound carriers to be controlled within wide limits.

The ferrite bead FP provided in the collector lead looks after RF interference.

Alignment is confined to setting the operating point. P3 is used to set 5.4V on the emitter of the transistor and the total current consumption is then about 10mA.

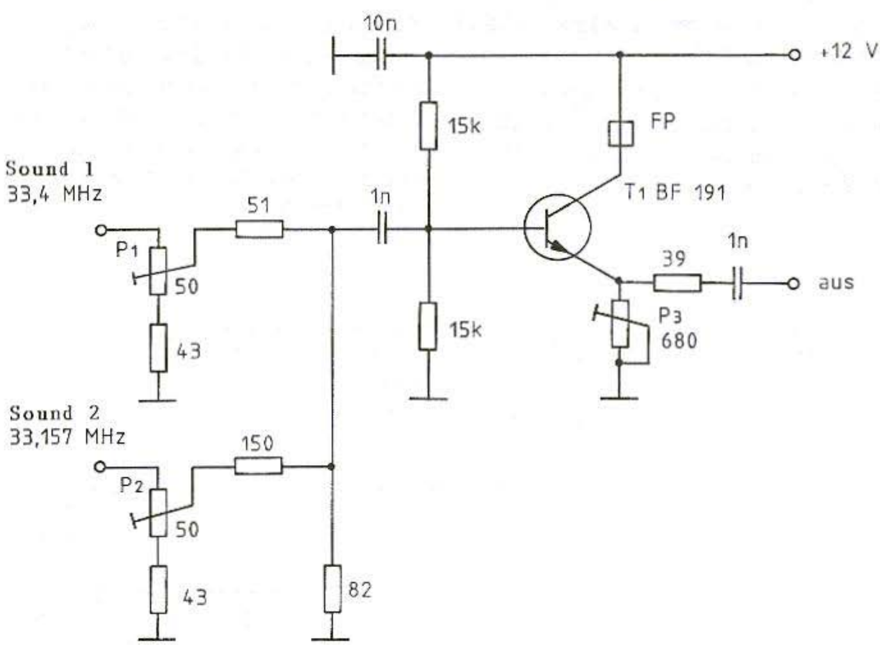

Fig.10: The Diplexer

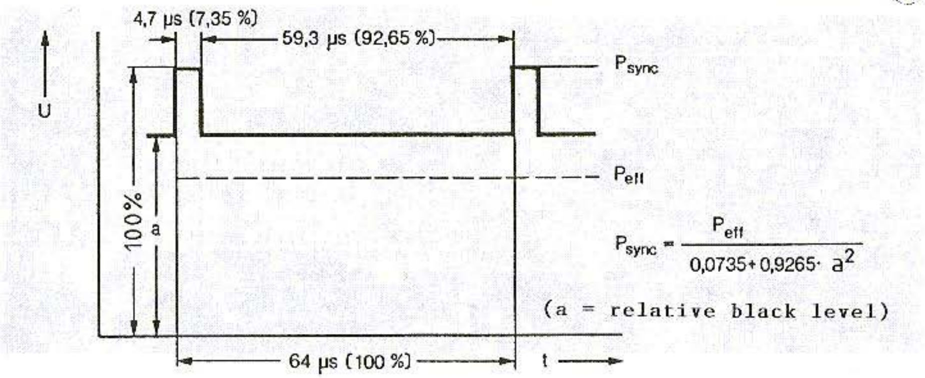

Fig.11: Relationship between Sync Power and Effective Power in a blackpicture

4.3 Qualitative Data

Presented in this section are some typical measured values of the modified 70cm ATV transmitter. Additionally a method is given at the outset for determining the peak sync power level.

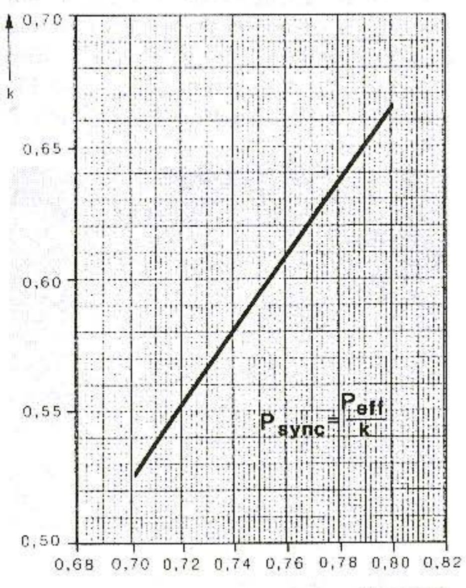

Fig.12: Correction Factors for calculating Peak Sync Power with black Vision Modulation

4.3.1Determining Peak Sync Power

Measurement of vision transmitter power - the peak sync power - is not as simple as for sound transmitters, since this power is available only for a brief period (Fig.11).

First thing to do is to measure the effective power of a defined signal (modulation of an all-black picture), for instance using a thermal power meter; then a correction factor for peak sync must be determined. Into this correction factor go the shape of video modulation and the size of the sync pulses.

The mathematical integration over one line

$$P = \frac{1}{T} \int_0^{64\,\mu s} u \cdot i \, dt$$

produces correction factors, as can be seen in Fig.12.

Also valid is:

$$P_{sync} = P_{eff} \cdot \frac{1}{0{,}0735 + 0{,}9265\, a^2}$$

$$= \frac{P_{eff}}{k}$$

where:

P_{sync} = peak sync power
P_{eff} = effective power
a = relative black level
 = 1- (sync length in % / 100)
k = correction factor

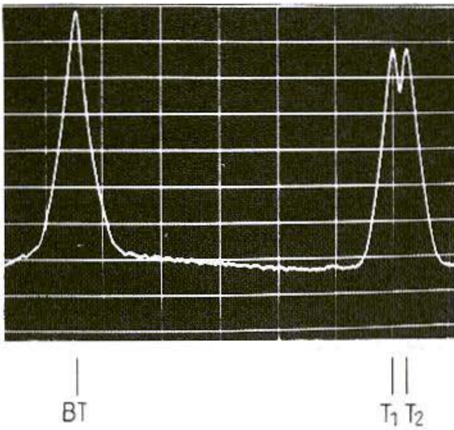

Fig.13: Picture to Sound Offset in both cases -13dB from the Vision Carrier (BT)

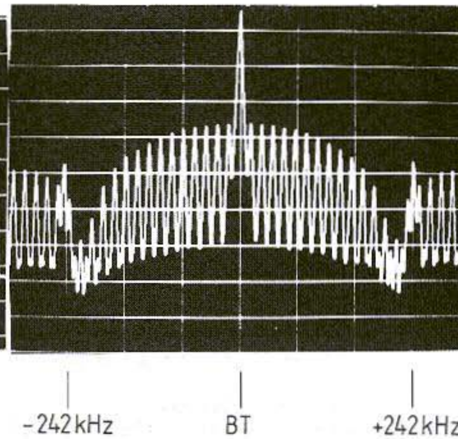

Fig.14: Cross-Modulation products +/- 242kHz from the Vision Carrier offset -48dB

To determine the length of the sync pulse I use my oscilloscope to display the demodulated video signal from my TV test/measurement receiver.

If we are working with vestigial carrier, I key in the video level for about 4 microseconds a zero blanking pulse. This allows the length of synchronisation to be determined exactly.

4.3.2Intermodulation

During the combined amplification of sound and vision signals additional sum and difference frequencies arise from the intermodulation between the shared frequencies. Within the channel in use these intermodulation products are designated cross-modulation, outside that channel as spurious signals.

Beyond the known intermodulation of the single audio transmitter, an additional intermodulation product manifests itself in a twin audio transmitter at the vision frequency plus and minus 242kHz (cross-modulation) and on the twin sound carriers at spacings of plus and minus 242kHz times n where n = 1, 2, 3, etc. - i.e. cross and spurious modulations.

Whereas the last are small enough to ignore, the cross-modulation on the vision carrier require increased vigilance since they can have an influence on picture quality. Measurements with varying vision to audio 1 and audio 2 carrier offsets produced discernible differences in the magnitude of these 242kHz products. First measurements (Fig's.13 to 15) were taken with vision to audio 1 to audio 2

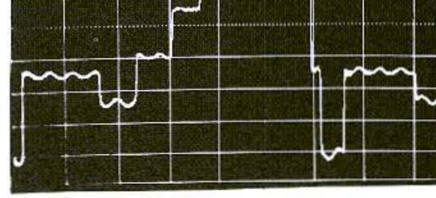

Fig.15: Cross-Modulation products shown on the demodulated signal in use (greyscale with zero blanking pulse)

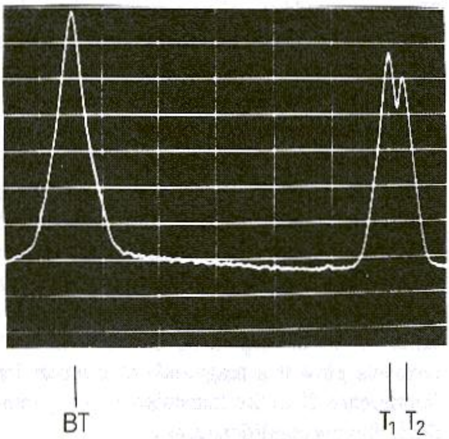

Fig.16: As Fig.13, but sound offset -13/20dB

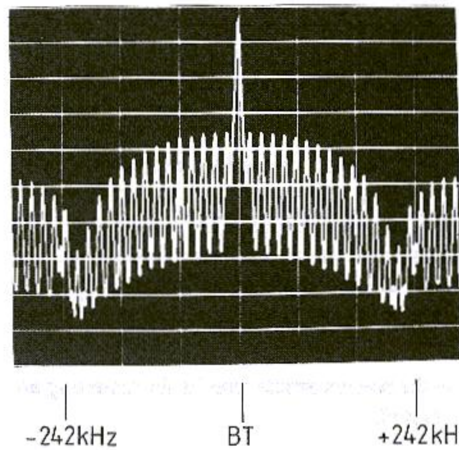

Fig.17: As Fig.14, but with significantly reduced cross-modulation products due to lower second sound carrier

(T1 and T2) offsets of -13dB each time, then with other offsets. A good compromise turned out to be offsets of -13 to -20dB, keeping cross-modulation down to -65dB, as seen in Figs.16 to 18.

Cross-modulation can also be seen very well in Fig.15 as an overlay to the useful video signal demodulated.

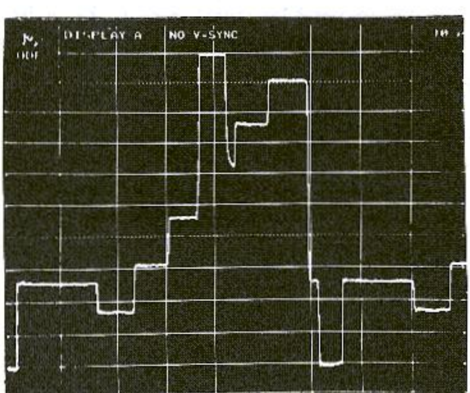

Fig.18: In comparison with Fig.15, the overlaying of the greyscale reduced

4.3.3 Difference Carriers-to-Noise Voltage Offset

As already mentioned, in the mixing of sound and vision carriers in the TV receiver the difference frequency of 5.5MHz (5.72MHz) takes on not only the modulated audio but also undesired, modulation-dependent phase variations of the vision carrier.

This interference contribution to the audio channels is measured modulating a test pattern and on a deviation of 50kHz procured with an audio modulation frequency of 500Hz.

This measurement must be carried out in an ''evaluated'' fashion, that is to say ahead of the measurement device a special filter (psophometric filter) is fitted.

Fig.19 shows the relevant evaluation curve and indicates that at a frequency of 1kHz the evaluation is 0dB. In addition the rectification of the quasi-peak must also be measured so that the interference effect of pulses can also be considered. Noise voltage offsets of -35dB are reached, at which the magnitude of the interference level is closely dependent on the power of the two audio carriers.

5. FUNDAMENTALS OF MATRIXING

The following discussions represent a small excursion into theory and included for the sake of completeness. They do not need to be considered in normal radio operation, but need to be considered and recognised when high-quality transmissions, such as for stereo, are to be achieved.

In the present article circuits for matrixing are omitted.

5.1 Matrixing in Radio Broadcasting

So that mono receivers with their single channel can retain both the information signals of a stereo transmission, FM radio matrixes in one channel the sum and in the other the difference of the two signals. In the stereo receiver the original information is de-matrixed or recovered by addition and subtraction (Fig.20).

If this technique is adopted for twin-audio transmission, a very high equality of channels is achievable but the channel separation is not quite adequate (slight crosstalk attenuation).

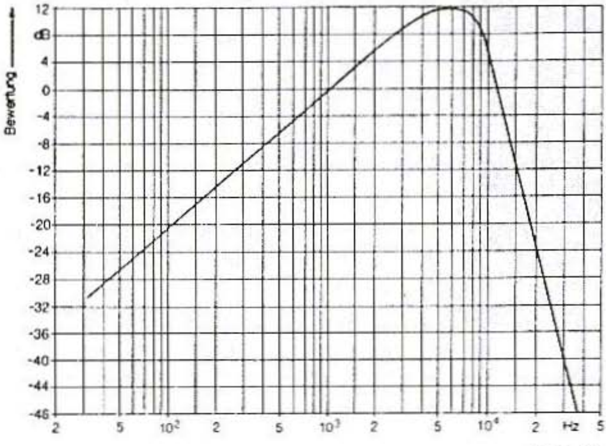

Fig.19: Evaluation curve for measuring the evaluated level of interference

There is an additional argument against this principle: as described, on the receiver side the intercarrier technique has been largely successful, with the sound IF achieved by mixing the vision and sound carriers. An (undesired) phase modulation of the vision carrier leads therefore via the sound IF to interference modulation in the two sound channels. A simple example calculation makes clear that the distribution of this buzz voltage over the channels following demodulation is to be expected. Given that both channels present a magnitude of intercarrier interference N to the transmission path, then the following conditions apply:

Channel 1

$$\frac{L+R}{2} + N \rightarrow \left[\frac{L+R}{2} + N\right] + \left[\frac{L-R}{2} + N\right] = L + 2N$$

Channel 2

$$\frac{L-R}{2} + N \rightarrow \left[\frac{L+R}{2} + N\right] + \left[\frac{L-R}{2} + N\right] = R$$

Transmission path Receiver

Through the formation of the sums and differences various interference magnitudes appear in both channels; in the extreme case the interference will appear at twice the level in the left-hand loudspeaker while the right-hand one would be undisturbed.

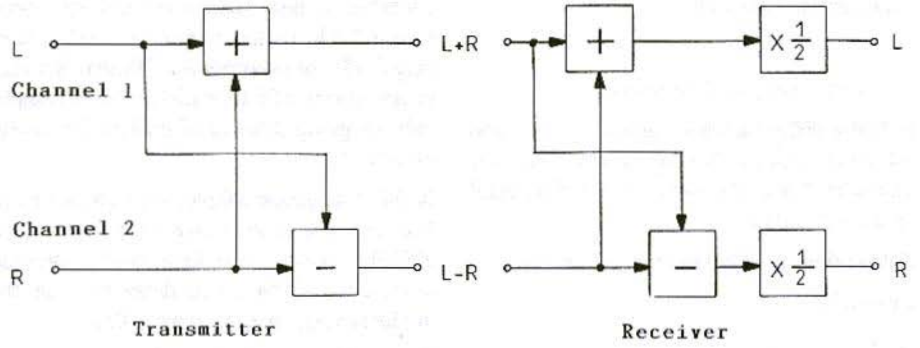

Fig.20: Matrixing in FM Radio

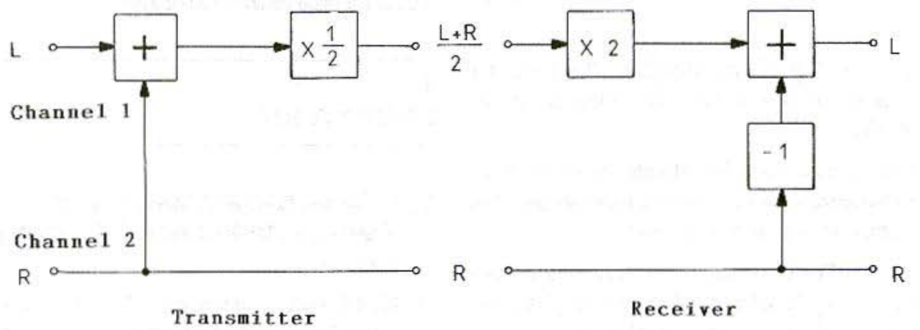

Fig.21: Matrixing in Television

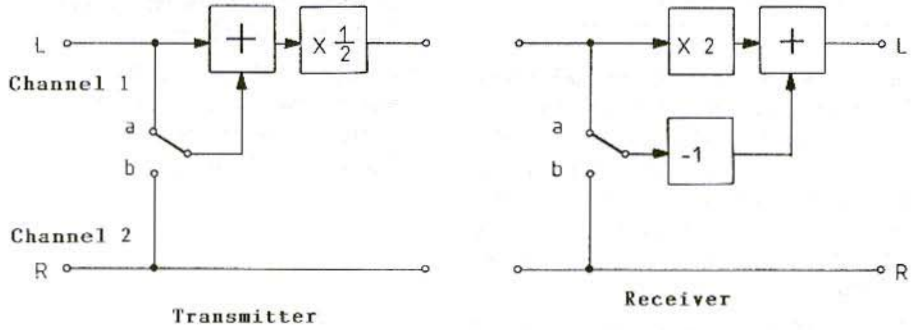

Fig.22: Matrixing with the changeover from twin-channel operation (a) and Stereo (b)

This technique is therefore excluded from television transmission.

5.2 Matrixing in Television

It looks different when instead of sum and difference signals, the signal of the sums is transmitted with the signal of the right-hand channel (Fig.21).

Calculation of the interference signal gives:

Channel 1

$$\frac{L+R}{2} + N \rightarrow [\frac{L+R}{2} + N] \times 2 + [-1(R+N)] = L+N$$

Channel 2

$$R+N \quad \rightarrow \quad = R+N$$

The halving of the signal of the sums on channel 1 serves only for equalisation of levels.

Both channels are thus affected in the receiver to the same extent, a major advantage over the technique described previously.

Finally Fig.22 expands the matrixing described in Fig.21 with simple switching between stereo and twin-audio transmission.

6. CLOSING REMARKS

The high occupancy of the amateur bands on the one hand and sensitive and highly selective receivers on the other, also paying heed to the handicap of standards means that the significance of accurate measurement is taking on ever more importance, both during home construction and afterwards in normal operation.

Methods of measurement for operational parameters such as power, intermodulation or deviation are adequately described in the amateur literature and are practised daily. The adoption of new technology (colour, twin-audio) leads to the introduction of further magnitudes of measurement. We can imagine measurements of differential phase and amplitude, of group delay or of differential carrier offsets.

In this connection simple, test signals or test lines can give good service. As an example, a 250kHz transient can very rapidly provide information about group delay time in the luminance region up to about 4MHz.

The ATV transmitter can be expanded in stages, allowing the group delay time to be adjusted and the characteristic line to be equalised. For the interested TV amateur this area presents a broad field of activity.

7. LITERATURE

(1) G. Sattler, DJ4LB: A Modular ATV Transmitter. VHF COMMUNICATIONS 1 and 2/73.

(2) H. Schwarz: Empfaengertechnik fuer das Zwei-Tontraeger-Verfahren. Nachrichten Elektronik 35 (1981), issue 4, pages 157 to 163.

(3) P. Dambacher, P. Singerl: Zweitonverfahren fuer das Fernsehen. Funkschau 17/1981, pp. 73/77.

(4) M. Aigner, R. Gorol: Eine Stereo-matrizierung fuer den Fernsehton. Rundfunktechnische Mitteilungen, 23. Jahrgang (1979), Heft 1, pp. 10-13.

Oliver Nell, Klaus Solbach DK3BA, Jochen Dreier DG8SG

Omnidirectional Waveguide Slot Antenna for Horizontal Polarisation Part-2 (conclusion)

3. ANTENNA FOR THE 23CM BAND

The requirement is an antenna that covers the complete 23cm band with the highest possible gain in the azimuth plane (horizontally).

With the help of a simulation (S-Compact) for matching and slot voltages and the additional simulation of the antenna diagram, an investigation was launched into how many elements should be used. To begin, equation 3 produces a maximum of 10 slot pairs with f = (1.3GHz - 1.24GHz) and f_0 = 1.27GHz. The simulation process indicated, however, that even with 12 slot pairs, VSWR did not pass significantly above 2 except at the extremes of the band. At the same time the beam squints downwards by about 1 degree at the bottom end and by the same amount upwards at the top end of the band. The related drop in gain including losses due to mismatching is about 1dB, whereas 12 dB_i is achieved in the centre of the band.

The antenna as completed is shown in Fig.8. For the waveguide a rectangular pipe 180 x 50 x 4mm (externally) to DIN 1770 standards is used (the material is AlMgSiv 0.5 F22); this is widely used as an extruded profile in mechanical construction. Producer is the company Wieland in Ulm, price about £7 per metre, maximum length 6 metres.

A flange is applied to the top end and screwed tight to form a short-circuit. Here at Telefunken we used a special salt bath welding process but for amateur technology a simple piece of sheet metal short-circuit will suffice, either screwed on or attached with conductive fastener (Fig.9).

The centre offset and length of the slots correspond with the results from examples 1 and 2. The distance of the slots from half or quarter of a wavelength of the waveguide (for short-circuit) were calculated with equation 5 for a centre frequency of 1.27GHz.

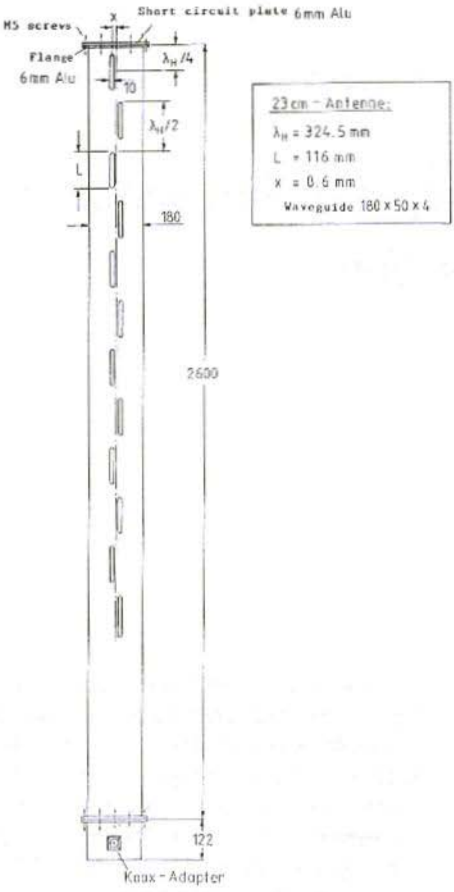

Fig.8: **Construction of the 23cm Antenna with 12 pairs of slots**

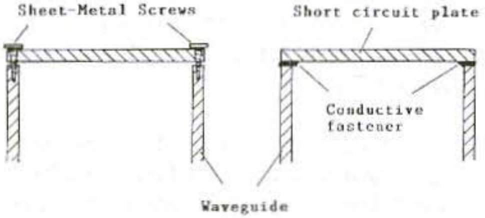

Fig.9: **Alternative possibilities for fastening the short circuit plates with screws or conductive fasteners**

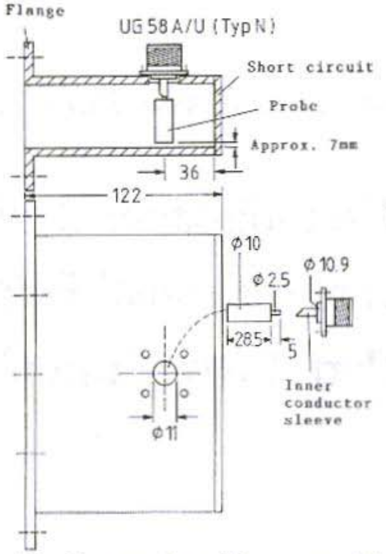

Fig.10: **Construction of the waveguide to coax transition of the 23cm antenna**

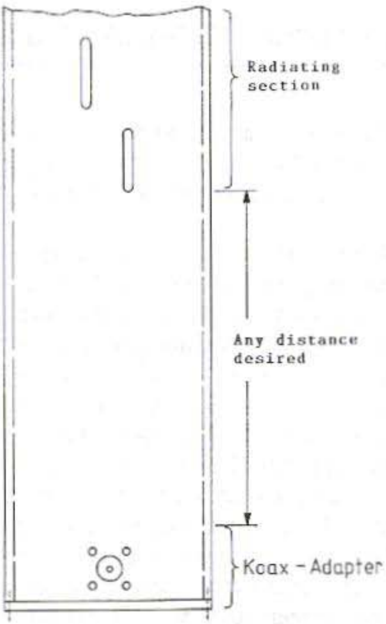

Fig.11: **Integration of the coax adaptor without flange connection**

Below the last slot there is a conductive section of about 65cm to a waveguide-to-coax transition at the end of the waveguide. The transition is made as shown in Fig.10, with a coupling probe protruding into the waveguide about an eighth of a wavelength from a short-circuit. The coupling probe comprises an N-connector with extended centre conductor. The connector is turned on the flange side around the outer coaxial conductor so that it can fit in a corresponding hole in the broad side of the waveguide. The inner conductor made into a sleeve is lengthened with brass circular section soldered onto it.

The dimensioning of this transition with its thickened probe and its short distance to the waveguide short-circuit is at variance with the conventional construction methods which use thin probes and a quarter waveguide wavelength distance. At the same time the matching bandwidth is well below the size of the full waveguide transitions, but with careful adjustment the complete 23cm waveband is achieved, with reflections attenuated by 30dB.

The transition can also be integrated directly into the antenna waveguide without a waveguide to flange connection (Fig.11). The antenna is then made up only of a single piece of waveguide with milled slots and the coaxial adapter together with a short-circuit plate at each end.

The complete antenna demonstrates the expected matching characteristic (Fig.12) with a VSWR less than 2 up to approaching the band ends and with the best match at the centre of the band. The radiation diagram (Fig.13) shows in the horizontal plane a variation of plus or minus 1.3dB. In elevation the first side-lobes appear at -13dB, as expected with an antenna with constant element levels, and the 3dB beamwidth is 6 degrees.

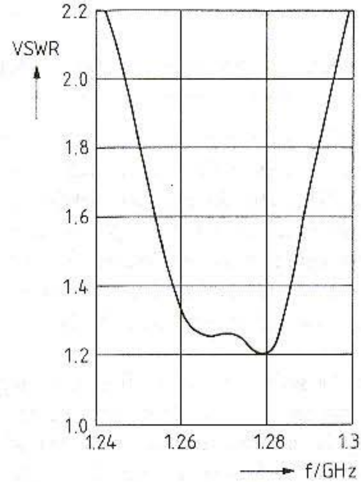

Fig.12: Measured SWR of the 23cm Antenna as a function of

The expected slight deviation of the beam (squinting) on leaving the centre frequency and the gain values given above were achieved with close approximation.

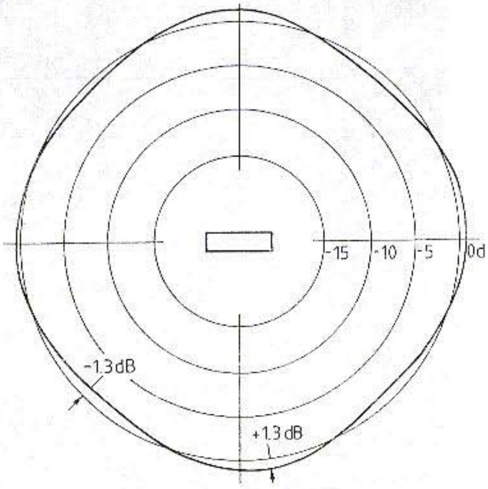

Fig.13: Measured Circular radiation diagram of the 23cm Antenna

4. ANTENNA FOR THE 13CM BAND

An ATV repeater required a horizontally polarised omni aerial on a frequency of 2392.5MHz. The dimensional details of the 23cm antenna can be scaled up if use is made of a waveguide cross-section which has been scaled down by the frequency relationship (the factor is 1.27 divided by 2.3925).

Sadly, the series of flat profiles according to DIN standard 1770 does not contain a rectangular section close to the result of the calculation performed on the 23cm profile. Therefore recourse was made to welding together two aluminium angle sections. Our limited production facilities were able to make a waveguide with the exact dimensioned cross-section of 86 x 21mm, but only in lengths of 900mm maximum.

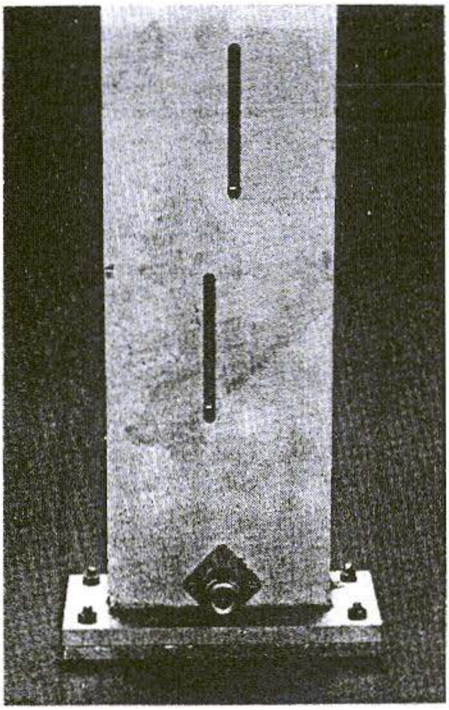

Fig.14: Photograph of the 13cm Antenna with 9 pairs of slots

With this length only nine slots can be undertaken and the slot dimensions must be re-calculated. The dimensioned slot conductor value according to equation 9 rises to:

$$Z_L/R = 1/9 = 0.111$$

Thanks to the exact scaling of the waveguide cross-section, the relationship of side a to b and the waveguide's wavelength to the free wavelength remain exactly as with the 23cm antenna. So the offset of the slot centre can be as in Fig.6 again. From Fig.6 we read off first $x = 9.75mm$ for $Z_L/R = 0.111$. With the scaling factor we get:

The slot length can also be taken from the corresponding 23cm drawing; Fig.7 gives initially for $x = 9.75mm$ the dimensioned slot length L/[lamda zero] = 0.494. At the design frequency the slot length thus becomes:

Incidentally the slot distances and the short-circuit distance emerge with the scaling factor from the corresponding values of the 23cm antenna. Because a 5mm tool was available conveniently, the slots were milled with this width.

Fig.14 shows the resulting antenna. The transition to coaxial conductor at the bottom end of the antenna is once more made with an N-connector and an extended probe. While the dimensions of the probe could be reduced to some extent by the scaling factor, the measurements of the connector itself naturally could not be changed. The cross-section of the coaxial line (connector) have only slight influence on the characteristics of the transi-

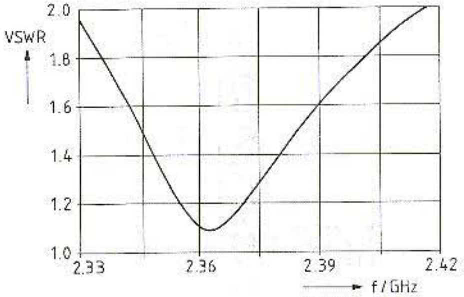

Fig.15: Measured SWR of the 13cm Antenna as a function of Frequency

tion, but on higher bands a smaller connector (for example an SMA) should be used in order to scale the relationships more closely. The short-circuit at the bottom end of the wave-guide is brought closer according to the scaling factor on the 23cm dimensions.

Measurement of the input matching of the antenna (Fig.15) shows a satisfactory match, though slightly shifted from the desired frequency - a sign that the rescaling was not 100 per cent successful. The elevation radiation characteristics (Fig.16) display a beam-width of around 8 degrees and between 13 and 14dB suppression of side-lobes. The measured antenna gain is around 10.4dB[i], within a few tenths of a dB of the theoretical value for the loss-less situation.

5. PRACTICAL EXPERIENCE

During 1989 and 1990 DG8SG/P was active from locator JN58BH in a number of contests and QRV on 23cm with SSB in BBT.

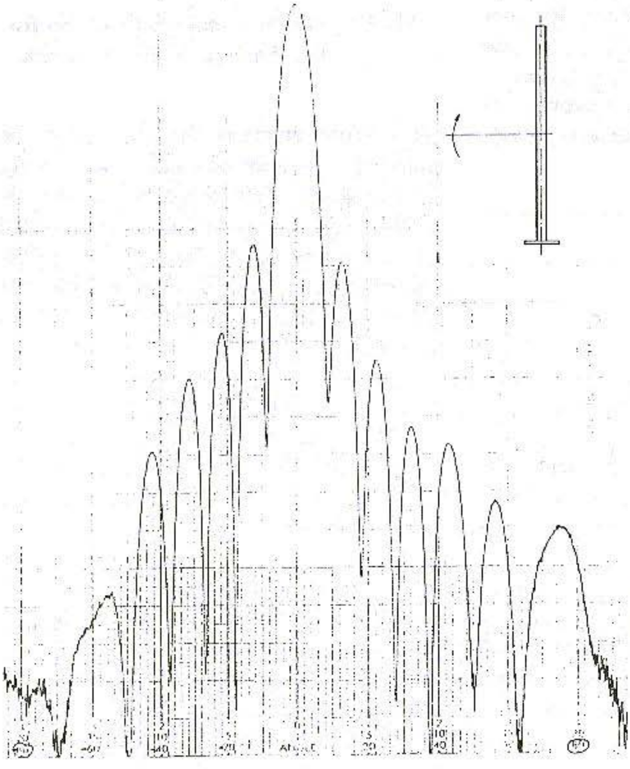

Fig.16: Measured elevationradiation diagram of the 13cm Antenna between -90 degrees (vertical to the ground) and +90 degrees (vertical upwards)

The matching he measured through cable losses of the feeder (1dB) appeared better than as measured in the laboratory.

As reference antenna a 23 element Yagi with 18.5dB[i] gain was available, fed via 10 metres of 5/8'' Flexwell cable. the omni aerial was connected to the transverter through 3.5 metres of RG-214 and a coaxial switch, enabling rapid selection of either antenna. On receive the Yagi showed an advantage (about 4 or 5dB) but only when it was accurately beamed. On transmit most stations reacted positively when both antennas were used (''the omni works fine'').

The 23cm and 13cm antennas were tested out on FM-ATV at the weather station tower of Gundremmingen power station (JN58FM). After solving problems of transport (the lift) and mounting (narrow platform) -the long 23cm antenna caused particular grief - the results were very satisfactory and got enthusiastic reactions (significantly improved picture quality over the original antenna system).

6. OUTLOOK

The experimental results support the validity of the dimensioning work. One can expect then that other, divergent sizes of antenna will be built. All the same, with slot totals significantly more than 12, a narrow bandwidth must be reckoned with and fine tolerances of waveguide size and slot distances will lead to frequency shifts. With amateur production methods antenna sizes of more than 20 to 25 elements should not be exceeded (approx. 3 degrees beamwidth). Smaller totals of slots will produce more broadbanded antennas and uncritical dimensional tolerances.

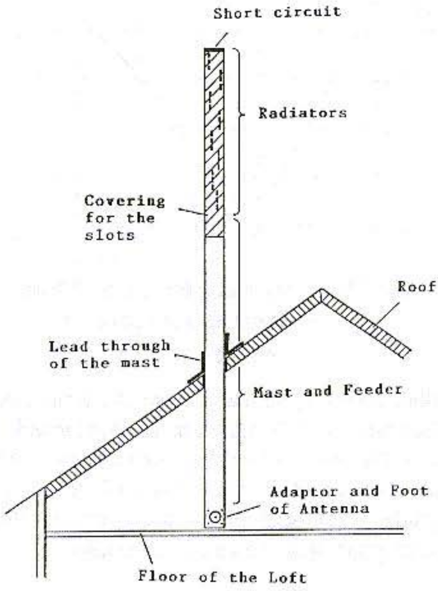

Fig.17: Practical mountingmethod for the Waveguide Slot Antenna

For outdoor antennas the slots must be protected, to prevent rain and snow entering the waveguide. Thin self-adhesive tape is suitable, e.g. Scotch Invisible tape, wound around the waveguide. The negligible thickness of normal tape will have no detectable influence on the slot characteristics at these frequencies.

Alternatively thin-walled plastic piping with low RF loss can be used to make a radome; suitable pipes will be difficult for amateurs to obtain and will additionally need its own method of fixing.

In both cases some ventilation is necessary at the bottom of the antenna to equalise air pressure and let out moisture.

Mounting can achieve an elegant unit of support mast, feedline and radiator all combined. This involves selecting a sufficient length of waveguide that will hold the radiating section (the slots) high enough, while the lower end with the coaxial input forms the lower fixing point or standing foot, as seen in Fig.17. In this way no separate feeder is required from the foot of the mast to the radiators: the extremely low feed loss of the waveguide at less than 0.1dB per metre could scarcely be achieved with coaxial cable!

In this form the antenna requires no bearer mast. On the contrary, the security of the rectangular pipe of the 23cm and 13cm versions should be sufficient to carry further antennas at the upper end. Their coax feeders can be led up the narrow side of the waveguide without problem and small screws and clips for fixing can be kept away from the radiating slots.

7. LITERATURE

(1) Ulf Huelsenbusch: 24cm Baugruppen, DUBUS 1/84.

(2) Oliver Nell: Kalibrationsnormale und Modenwandler in Hohlleitertechnik, Hohllleiterschlitzantenne fuer Rundumstrahlung. Diplomarbeit (2 Teile) Fachhochschule Giessen/Friedberg (Prof. Dr.-Ing. Mehran) Telefunken Systemtechnik, Ulm (Dr.-Ing. Solbach)

(3) T. Takeshima: X-Band omnidirectional double-slot array antenna. Electronic Engineering, October 1967, pp. 617-621.

(4) S. Siver: Microwave Antenna Theory and Design, McGraw-Hill, 1949.

Bernd Bauer DF1YW

A DTMF Converter with Multiple Switching Outputs

The author describes a DTMF converter which uses the dual-tone sequence received to control any desired on or off switching of up to six outputs. Using a three-level address which can be defined by the user, it is possible to operate up to 4,096 devices independently of one another on the same frequency.

The circuit would be relatively difficult to realise using normal devices but has been achieved using custom Generic Array Logic chips.

1. INTRODUCTION

Many modern pieces of radio apparatus can send DTMF (dual-tone, multi-frequency) tone sequences. In the USA these tones are used for dialling into the telephone system and permit direct dialling into the public telephone system.

This function has generally less practical use on sets imported for the European market since unlike the USA, connection between amateur radio and the public telephone system is not allowed.

Another possible use of the DTMF tones lies in the remote control of various devices. The reception and decoding of the transmitted tone sequence using the circuit described now enables the control of various switching outputs. A total of six separate outputs can be operated independently of each other.

The operation of the desired switching output is carried out following reception of the three-digit address defined by the user. The fourth digit sent actually switches on or off. The switching is permanent, that is it remains in the switched position until power is removed or the outlet is switched off.

According to the type of IC7 used, all switching outputs can be active High or Low (74LS06) or also have Open Collector outputs (74LS05).

Radio sets not fitted with a DTMF keypad can still be used with the assistance of a so-called Tone Dialler Pad of the type sold cheaply for remote controlling answering machines and so on. The desired tone sequence can then be coupled acoustically to the microphone of the radio.

1.1 Format of the DTMF system

The DTMF scheme uses a total of eight different audio tones. The frequencies of the four lower tones are below 1kHz in the so-called Low Group, while the other four tones are in the High Group above 1kHz. When a DTMF tone-combination is sent, always one tone from the Low Group and one tone from the High Group are transmitted together. There are thus 16 combinations. Table 1 shows the relationship between the keys and the transmitted frequency pair.

Most of the available DTMF transmitters support only 12 of the 16 possible keys; the combinations A, B, C and D are normally unused.

2. CONTROLLING THE CONVERTER

As already mentioned, the converter responds after receiving a code address, which the user programmes on the PCB using DIP-switches. Table 1 shows the relationship between the DTMF key combinations and the frequency pairs transmitted, also the logic state resulting on outputs Q1 to Q4 of the DTMF receiver (IC1). Corresponding to these logic states, the DIP-switches provided on the board preset the desired card address. SW1 thus sets the first digit of the address. Fig.2a indicates the setting of the DIP-switches for the card address 7 8 0.

After receipt of the first step of the address, the next step must be received within one

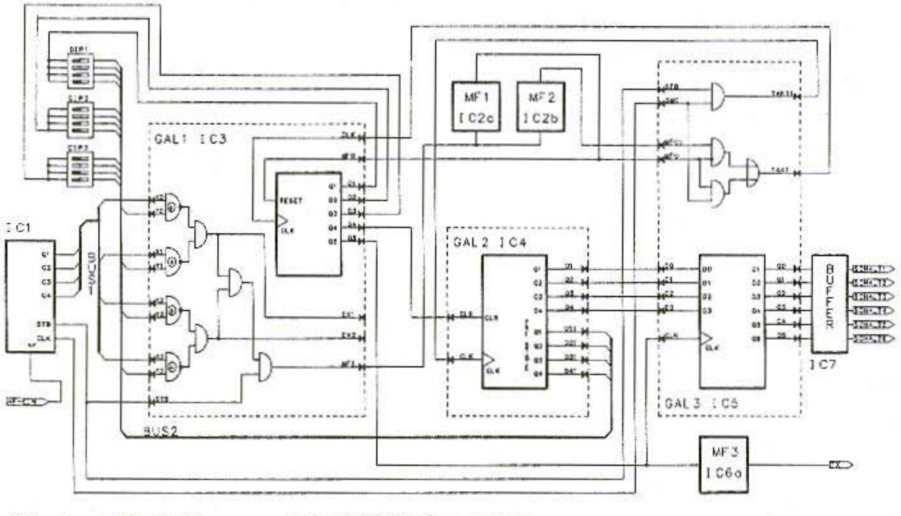

Fig.1: Block Diagram of the DTMF Converter

Key Number	F_{LOW} Hz	F_{HIGH} Hz	Q4	Q3	Q2	Q1
0	941	1336	1	0	1	0
1	697	1209	0	0	0	1
2	697	1336	0	0	1	0
3	697	1477	0	0	1	1
4	770	1209	0	1	0	0
5	770	1336	0	1	0	1
6	770	1477	0	1	1	0
7	852	1209	0	1	1	1
8	852	1336	1	0	0	0
9	852	1477	1	0	0	1
*	941	1209	1	0	1	1
#	941	1477	1	1	0	0
A	697	1633	1	1	0	1
B	770	1633	1	1	1	0
C	852	1633	1	1	1	1
D	941	1633	0	0	0	0

Table 1: Relationship between DTMF keypad numbers, DTMF frequency and the resulting logic state on Q1 to Q4 (IC1) of the DTMF Receiver

second. If this is not the case, the address is declared invalid and the code input must be made afresh.

After receipt of the third step of the address, any subsequent digit other than A, B, C or D leads to a switching process. The relationship between a key and the process carried out is given in table 2.

3. CIRCUIT

To save on component count, the major part of the circuit employs GAL (Generic Array Logic) devices. These are building blocks which can be programmed by the user. As well as switching networks (the coupling of several inputs by logical operations), it is possible also to realise switching functions (recursive networks, such as counters).

Determining the function of the GAL is done with logical equations, which describe the relationship between input variables and the related output variables. With the relevant program and a suitable programming device, the GAL can then be programmed.

3.1 Block diagram

With the aid of the block diagram in Fig.1, the function of the complete circuit can be described.

In the three boxes drawn dotted, the logic implemented in the GAL is to be found. In GAL1 (IC3) this includes an address comparator plus a ring counter which is resettable via a Reset input. In the reset state Q1 is High and Q2 = Q3 = Q4 = Q5 = Low.

In GAL2 (IC4) we have a binary counter, also resettable, this time via a Clear input. In addition to outputs Q1 to Q4, w e have another set Q11 to Q14 which behave identically to

Key	Switch Status
0	Switch 1: OFF
1	Switch 1: ON
2	Switch 2: OFF
3	Switch 2: ON
4	Switch 3: OFF
5	Switch 3: ON
6	Switch 4: OFF
7	Switch 4: ON
8	Switch 5: OFF
9	Switch 5: ON
*	Switch 6: OFF
#	Switch 6: ON

Table 2: Relationship between DTMF key and the resulting switch condition

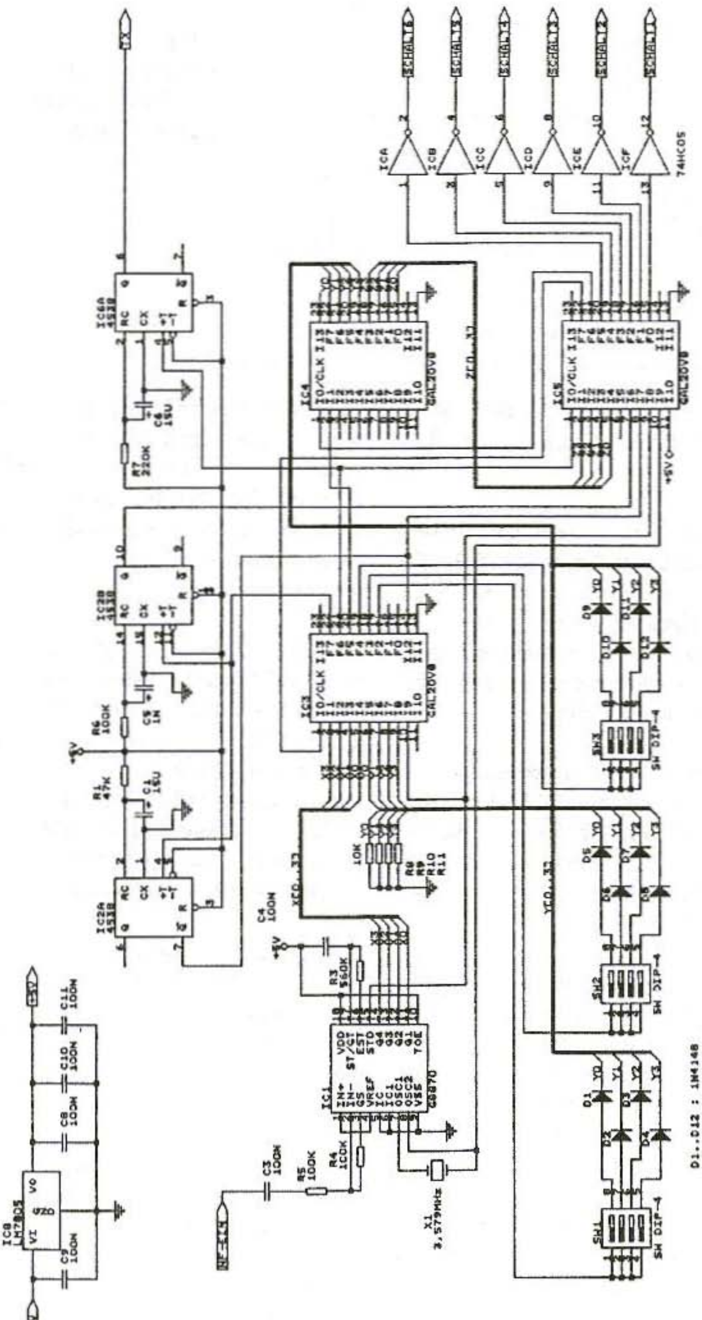

Fig.2: Circuit of the DTMF Converter

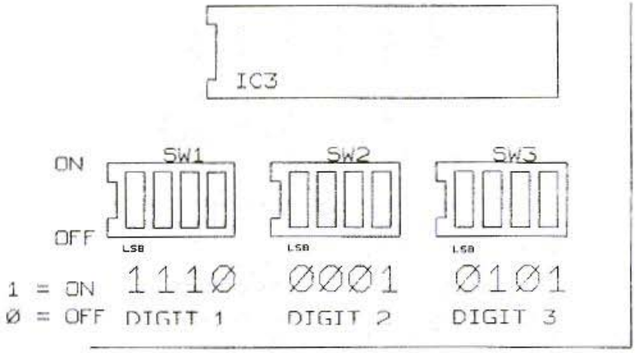

Fig.2a: Setting of the DIP-switches for card address 780

Q1 to Q4 up to the stage where they can be made Tri-State by a Low signal on the Clear input.

In GAL3 (IC5) there is an output register which, corresponding to the status of D0 to D3 with a positive pulse edge on CLK, writes either a High signal or a Low signal to the switching outputs Q0 to Q5. Additional logic in this chip is represented by the logic symbols indicated on the diagram.

The blocks MF1 to MF3 represent monostables. IC1 is the integrated DTMF receiver circuit which writs a four-bit word on the Bus according to the tone combination received. A High signal on the STD-output of the IC indicates a valid data word.

In the initial state after power is applied, 3MHz clock pulses are present at the clock input of GAL1, resetting the counter continually since the Reset input is High. As a result Q1 (GAL1) is High and the four-bit wide data word determined by the DIP-switch (DIP1) is applied to Bus 2.

The word on Bus 2 is compared in the address comparator of GAL1 with the data word on Bus 1 carrying the DTMF values received.

If the two data words are identical, then (assuming STB is High = valid data word) output MF1 goes to High potential. The rising edge of this signal triggers the following monostable MF1 for about 1 second to Low potential. With this the counter in GAL1 is cleared via its Reset input and the somewhat delayed positive pulse edge in MF2 sets Q2 High and Q1 Low.

The High potential on Q2 causes the data word on DIP2 to be transferred to Bus 2. If a valid DTMF data word from IC1 arrives before MF1 has changed back to High, then MF1 is retrigered and Q3 in GAL1 changes to High potential. With this the data word from DIP3 is put on Bus 2. If no DTMF data word comes from IC1 before MF1 goes High again, then the counter (GAL1) is reset.

After receipt of the third valid signal the counter in GAL2 is cleared by its CLR input. At the same time the tri-state outputs Q11 to Q14 become active and transfer the counter status of the counter in GAL2 to Bus 2.

The STB signal of the fourth DTMF data word effects an upwards count of the counter in GAL2 until the data words on Bus 1 and Bus 2 are identical.

When both data words are identical, Q5 of the counter in GAL1 goes High on the positive pulse edge of MF1 (GAL1). With this the register in GAL3 takes over the state of the

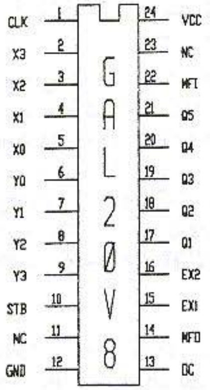


```
/q1 :=  q4*/q5*/q2*/q1*/q3*/mfo
        + q2*/q1*/q4*/q5*/q3*/mfo
        + q1*/q2*/q3*/q4*/q5*/mfo
        + q3*/q1*/q2*/q4*/q5*/mfo
q2 := q1*/q2*/q3*/q4*/q5*/mfo
q3 := /q1*q2*/q3*/q4*/q5*/mfo
q4 := /q1*/q2*q3*/q4*/q5*/mfo
q5 := /q1*/q2*/q3*q4*/q5*/mfo

ex1 = /x0*/y0*/x1*/y1+/x0*/y0*x1*y1+x0*y0*/x1*/y1+x0*y0*x1*y1
ex2 = /x2*/y2*/x3*/y3+/x2*/y2*x3*y3+x2*y2*/x3*/y3+x2*y2*x3*y3

mfi = ex1*ex2*stb
```

Fig.3: Connections and logical expressions for GAL1 (IC3)

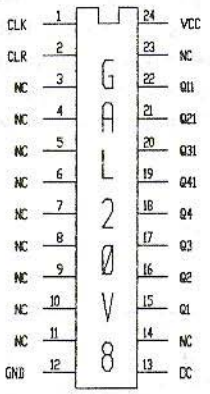


```
q1 := /q1*q2*clr + /q1*/q2*clr
q2 := q1*/q2*clr + /q1*q2*clr
q3 := /q1*q2*q3*clr + /q2*q3*clr + q1*q2*/q3*clr
q4 := q1*q2*q3*/q4*clr + /q1*q2*q4*clr + /q2*q4*clr
      + /q3*q4*clr

if (clr)
q11 = q1
if (clr)
q21 = q2
if (clr)
q31 = q3
if (clr)
q41 = q4
```

Fig.4: Connections and logical expressions for GAL2 (IC4)

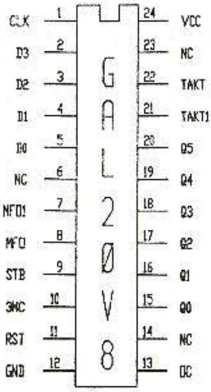


```
q0 := d3*/d2*d1*/d0*rst + q0*/d0*rst + q0*d1*rst
      + q0*d2*rst + q0*d3*rst
q1 := /d0*d1*/d2*/d3*rst + q1*/d0*rst + q1*/d1*rst
      + q1*d2*rst + q1*d3*rst
q2 := /d0*/d1*d2*/d3*rst + q2*/d0*rst + q2*d1*rst
      + q2*/d2*rst + q2*d3*rst
q3 := /d0*d1*d2*/d3*rst + q3*/d0*rst + q3*/d1*rst
      + q3*/d2*rst + q3*d3*rst
q4 := d3*/d2*/d1*/d0*rst + q4*/d3*rst + q4*d2*rst
      + q4*d1*rst + q4*/d0*rst
q5 := d3*/d2*d1*d0*rst + q5*/d3*rst + q5*/d2*rst
      + q5*d1*rst + q5*d0*rst

takt1 = 3mc*stb
takt = mfo1*/mfo+3mc*mfo
```

Fig.5: Connections and logical expressions for GAL3 (IC5)

outputs Q1 to Q4 of the counter in GAL2. The data acquired controls one of the six outlets (Q1 to Q6) of the register in GAL3, according to the data word received, either to High or Low potential (table 2).

The pulse on the clock input of GAL3, which transfers the state of the counter in GAL2 to the output register in GAL3, triggers monostable MF3. The output signal of MF3, with a duration of about 2 seconds, can be used as a confirmation sign of a successful write process to the output register of the DTMF converter.

The switching outputs of the register in GAL3 are buffered by open collector inverter IC7 (73LS05).

3.2 Circuit diagram

The complete circuit diagram of the DTMF converter is shown in Fig.2. The heart of the circuit is the DTMF receiver (IC1). This transforms the received audio signal into four-bit data words.

The relationship between the received tone pair and the data word produced is given in table 1. The audio sensitivity of IC1 is set by the relationship of R4 to R5.

The combination of R3 and C4 forms a time constant which determines the minimum time that a DTMF tone pair must be received in order to be recognised as valid. Security against false triggering by speech can be increased in this way. That said, even with very short time constants no false results were detected.

The diodes D1 to D12 on the DIP-switches SW1, SW2 and SW3 are to prevent short circuits between the switches.

4. PROGRAMMING THE GAL CHIPS

A universal programmer is used for programming the GALs. With the relevant device-specific software the logical expressions can be transformed into a so-called fuse map. Since this software is different for every programmer, just the logic expressions and the connections of the GAL used are given (Fig's.3, 4 and 5).

The function of the GAL used is described clearly by the connections employed and the logic functions implemented.

The symbol * is used here to indicate the logical AND function and + logical OR connection. The oblique slash of a term indicates its negation. The assignment operator := indicates a combining output, i.e: a register output.

5. LAYOUT

The layout of the circuit developed here was restricted to a size of 55.5 x 74mm. This was to enable the use of a commercial sheet-metal casing.

Fig.6 shows the solder side of the PCB and Fig.7 the component side. In this compact construction form, all diodes, resistors and crystals are placed vertical. For setting the card address low-cost DIP-switches are suitable.

The connector strip ST1 carries the switching outputs, a ground connection and also the signal TX. The audio input is next to C3 beneath IC1. Fig.9 gives an impression of a completed sample.

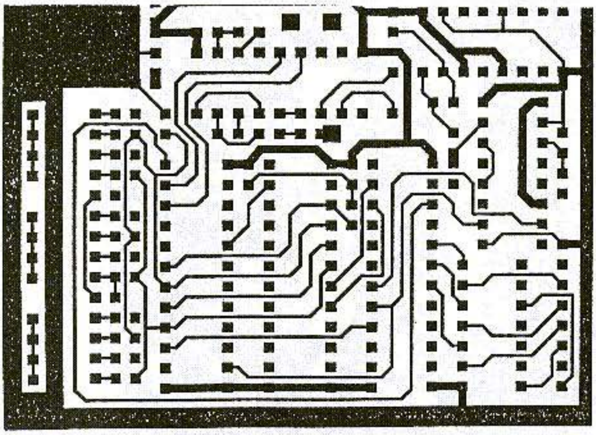

Fig.6: DTMF Converter Layout, solder side

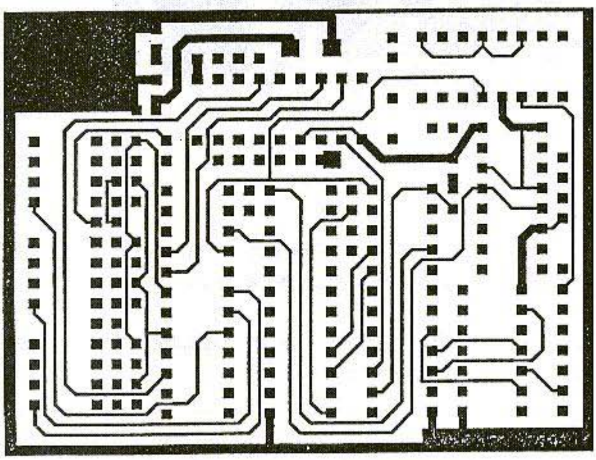

Fig.7: DTMF Converter Layout, component side

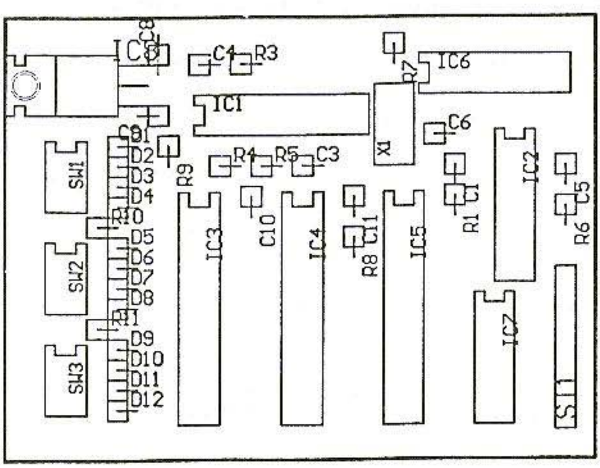

Fig.8: DTMF Converter, component layout

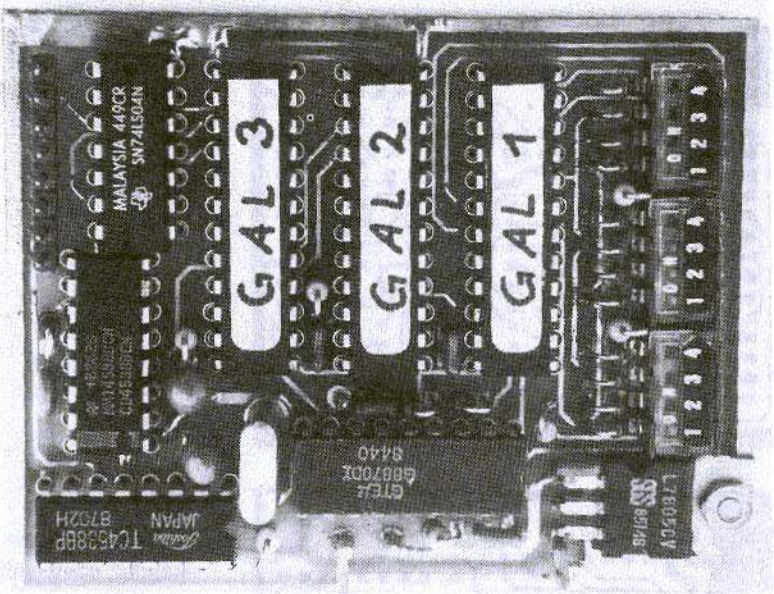

Fig.6:A Constructed Sample

6. LITERATURE

(1) CRYSTAL Semiconductor Corporation: Analogue Data Book, data sheet CS8870, pp. 4-23.

(2) Radio Amateur's Handbook 1982: A home-made touch-tone encoder, pp. 13-23.

(3) National Semiconductor: data sheet GAL20V8A, 4/89.

Dr.Ing. Ralph Oppelt DL2NDO (ex DB2NP)

Universal 2:1 Economy Transformer for DC Part-2 (conclusion)

5. SOME NOTES ON ASSEMBLY

The assembly of the DC converter as per the board fitting plan in Fig.4 should in fact pose no problems, as long as a low frequency circuit is involved.

A single-sided layout was chosen so that the board could be manufactured simply and cost-effectively. Four wire bridges must be taken into account for this, and it would be best to fit them first.

Those wishing to make their own boards should use base material with a 70 um. Cu coating or should take an otherwise normal board with a 35 um. coating thickness and thickly tinplate the current paths in the switching section.

The pin configuration of the ferrite core has been selected in such a way that, even if the core is rotated through 180 degrees, the connections fall back into their paths, so that fitting errors are impossible. As regards the other structural elements too, as far as possible only those of the same type have been selected, in order to avoid any chance of error.

Thus, for example, almost all the resistances have the value 9k1 (10k is also possible), almost all the Zener diodes are 16V, almost all the capacitors (apart from the electrolytic capacitors) have a value of 100nF, and so on, which further increases the simplicity of assembly.

Before using the equipment for the first time, it is recommended that you do not initially equip the MAX 626 driver and that you test the square wave signals at their inputs (pins-2 and 4) if the converter is operated as a doubler and is powered by a U voltage of about 10V. You should then be able to measure two square waves, overlapping by about 2us, with a period of approximately 66us.

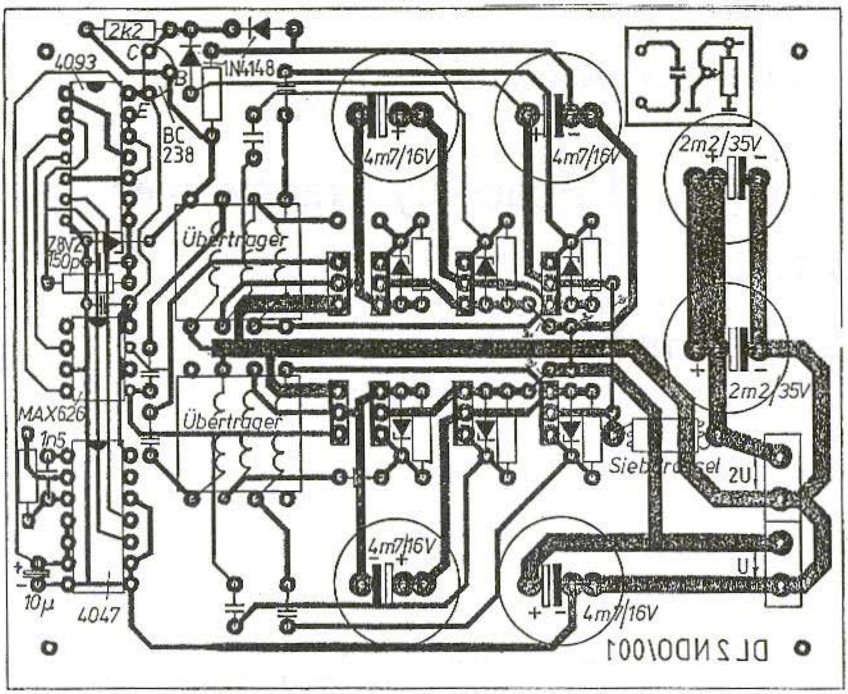

Fig.4: Component Overlay for the Voltage Converter

5.1. Notes on the components

T1 to T8:	BUZ 11, BUZ 12 (Siemens) or equivalent BUK types from Philips
T9:	BC 238 or similar
All diodes:	1N4148 or similar Si diodes
All Zener diodes:	400mW types
All resistors:	1/4 W, RM10
Tr1, Tr2:	Ferrite core E 16/5 or L, material N27 (Siemens B66307-G-X127) with coil bodies and clips: 3 * 80 Wdg., trifilar winding, 0.2 CuL
Dr:	Valvo FXC-3B-2.5 wide band chokes (six core)

6. RESULTS ON SPECIMEN CONSTRUCTIONS

For a practical trial, two specimen units were constructed, which differed only in their switching transistors. In one case the Philips type BUK453 was used, which essentially corresponds to the Siemens type BUZ10. In the other case, the low resistance Siemens type BUZ11 was used.

Fig.5, then, shows the efficiency values obtained for these two specimens in doubler mode, with an output current of up to 3 A and an input voltage of 15 V. The measuring equipment used to determine currents and voltages was a 5 & 1/2 digit multi-meter with a basic accuracy of < 0.01%. The calculated curves from Fig.2 are shown here again for comparison.

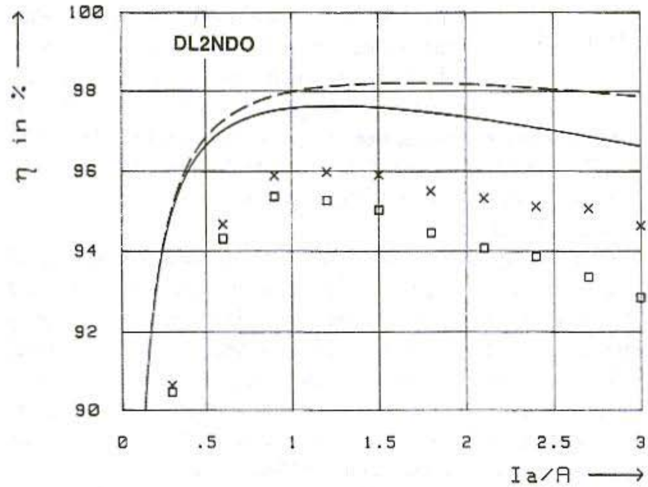

Fig.5: Measured Efficiency in Doubler Mode at U = 15V Input Voltage
Square - fitted with BUK453 (= BUZ10)
X - fitted with BUZ11
In addition, the associatec calculated curves of Fig.2, for which, of course, ideal, loss-free capacitors were assumed, have been drawn in.

The measured and the corrected curves are essentially similar. Of course the measurement brought out approximately 2 to 3% of values which were not so good. This is essentially due to the fact that in the calculation the (unknown) losses of the capacitors were ignored and also all lines were assumed to be ideal. If a mere 0.16 ohms more are added to R in equation 4 and a slightly higher basic power loss is assumed, the corrected curves run practically along the exact path of the measured curves.

Since only standard electrolytic capacitors were used in the specimen units, this minimum increase in the resistance can safely be taken as a starting point. If special (low ESR) switching network electrolytic capacitors are used (although they are several times dearer), the gap between the theoretical and the measured curves in Fig.5 proves to be significantly smaller.

The measured static internal resistance - analogously to the discrepancy in the efficiency curves - is also approximately 0.16 ohms higher than the value determined in part-1 as per equation 4.

The basic power loss assumed in Fig.2, part-1 is based on the following static current measurement (I_r = input static current):

Operation	U or 2U	I_r	P_0
Doubler	5 V	20.0 mA	100 mW
Doubler	10 V	31.2 mA	312 mW
Doubler	15 V	42.4 mA	636 mW
Bisector	10 V	10.0 mA	100 mW
Bisector	20 V	15.6 mA	312 mW
Bisector	30 V	21.2 mA	636 mW

The basic power loss, P_o, is thus independent of the individual type of operation. As Fig.5 further shows, the maximum converted power was approximately Since no cooling bodies of any type are provided, this power can, of course, be transferred only with the BUZ11 in continuous operation (up to I_a = 3.5 A, i.e: P_a = 100 W), and the BUK453 also manages continuous output currents of approximately 2 A. If cooling bodies are used, much higher output currents can certainly be obtained. But we then find ourselves in an area in which the efficiency becomes progressively worse, so that it makes more sense to use low-resistance MOSFETs instead.

7. APPLICATIONS AND FURTHER DEVELOPMENTS

On the basis of the universal characteristics and the high efficiency of this "DC voltage transformer", there is an extremely wide range of applications, in particular for mains-independent power supplies, and thus anywhere where accumulators, batteries or even solar energy cells provide the source of energy. We are thinking here of typical "tuning problems" in mobile radio, when, for example, a standard 12 V radio apparatus has to be used with the 6 V accumulator of a "Trabbi" or with the 24 V network of a lorry, or even, once, a 24 V final stage used with a 12 V source. In each case, one and the same module can bring about the voltage conversion required. The power MOSFETs used merely have to be tuned to the maximum required output current.

Of course, the voltage converter has other uses than as a doubler or bisector with a common negative pole. If, for example, point c in Fig.1 is selected as common earth, the output voltage -U, between point b and the earth is available in operation as a bisector, i.e: you have a bisector with a common positive pole.

Similarly, the voltage converter module can be used as an inverter, a symmetriser, etc. When it is operating as an inverter, point b in Fig.1 represents the common earth, so that a positive output voltage, U (from point c to b) is obtained from a negative input voltage, U (from point a to b). Thus both polarities are available. When the module is used as a symmetriser, as when it is operating as a bisector, make sure that only point b acts as the common earth. Thus, from the input voltage, 2U, we obtain the voltages +U and -U. The power loss ratios, of course, are completely different here to those for standard doubler or bisector operation. If, for example, a purely symmetrical load is available when the module is being used as a symmetriser, there is practically no power loss in the switches. The power loss depends rather on the degree of asymmetry of the load. But these peculiarities were deliberately not examined more closely in part-1.

For operation in the immediate vicinity of amateur radio installations, it is recommended that the board be built into a high-frequency tight housing in all cases, so that no reciprocal interference can arise due to beam effects. When solar power cells are connected, the usual protective measures should naturally be taken for the buffer accumulator (total discharge protection, reverse current interlock, etc.). Pay special attention here to ensuring that the module works in both directions!

Electronic protection against battery reversal, short?circuits, over-voltage, etc. is naturally also conceivable. But it was decided not to go into these additional areas, because, in the first place, the switching scope increases and the construction costs go up with it, in the second place it always involves a certain loss of efficiency, and in the third place the need for one or another extension depends on the individual application. Individuals should decide for themselves whether they want to add this or that on externally. There are already sufficient examples of electronic protection circuits available in the relevant literature.

8. LITERATURE

(1) U.Tietze, C.Shenk (1980): SemiConductor Circuit Engineering 5th edition, Chapter 18.5., pp. 583 ff. Springer?Verlag, Berlin

(2) As (1), but corrected reprint of 3rd edition (1976) Chapter 4.5., p. 37

Index of Volume 23 (1991)

Article	Author	Edition	Pages
AMATEUR TELEVISION			
An FM ATV Receiver for the 23cm Band	Wolfgang Schneider DJ8ES	1991/1	3 - 15
10GHz ATV The Easy Way, Part-1	Jim Toon, G0FNH	1991/1	43 - 46
10GHz ATV The Easy Way, Part-2	Jim Toon, G0FNH	1991/2	102 - 106
Modifications of the FM-ATV Transmitter DD2EK 002. Increasing the Output Power to 50mW	Wolfgang Schneider DJ8ES	1991/3	158 - 159
ATV with twin Sound Channels, Part-1	Rainer Tappert	1991/4	194 - 199
10GHz ATV The Easy Way, Part-3	Jim Toon, G0FNH	1991/4	220 - 228
DSP TECHNIQUES			
DSP Computer Update No.1	Matjaz Vidmar, YT3MV	1991/3	147 - 157
Simple Doubling of the Data Storage Capacity of the DSP-Computer	Heinz Kriegelstein	1991/4	206 - 210
2 M BAND			
Universal Transverter Concept for 28, 50 & 144MHz	Wilhelm Schuerings DK4TJ Wolfgang Schneider DJ8ES	1991/3	175 - 187

Dr.Ing. J.Jirmann DB1NV

A Tracking Generator for the DB1NV Spectrum Analyser

In previous issues, a spectrum analyser for amateur use was described in these pages step by step.

Some readers have now asked how far existing functions, such as a broad-band adjustable, although thanks to a connectible PLL, a more stable oscillator, calibrated tuning and sweep, together with digital image storage with print-out facility, can now be incorporated for a "better" sweep generator.

The result of this further development, a tracking generator for the 0 to 450 MHz frequency range, is described below.

This provides a sweep test rig with a measurement dynamic range of more than 60 dB and high stability, so that narrow-band sample objects such as quartz filters can also be measured.

1. LIMITS OF CONVENTIONAL SWEEP MEASUREMENT ENGINEERING

If, for example, you want to investigate the frequency behaviour of a selective preamplifier using a wobbulator, the procedure is as follows. The sweep generator is connected to the amplifier through an adjustable damping element (usually built into the wobbulator). A suitable detector is connected to the amplifier output and the detector's DC signal controls the Y channel of the sweep display unit. With this process, you can come up against several problems which are not immediately apparent:

➡ The HF frequency selected should be low enough to ensure that the amplifier is not overloaded; an amplifier output level of between -10 and 0 dBm usually represents the limit.

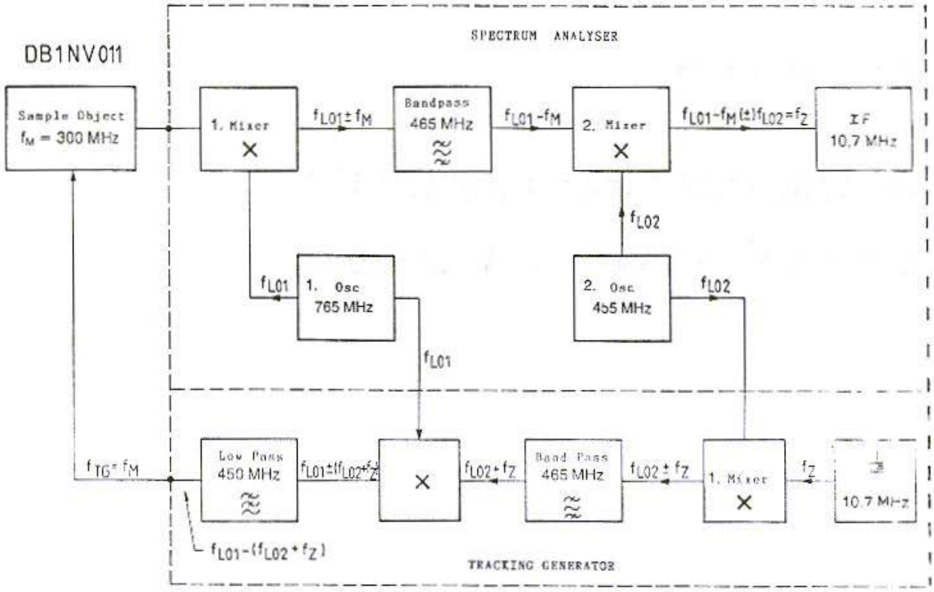

Fig.1: The Spectrum Analyser and Tracking Generator

➡ The output voltage of a diode detector in this range below -10 dBm is approximately proportional to the HF output, so that a level range of, at best, only 20 dB is displayed on the display unit. Even using "logarithmic amplifiers" between the detector and the display unit scarcely extends the range of signal detection to below -50 dBm.

➡ The wide-band detector can not differentiate between the useful signal and the harmonic waves or interfering signals stemming from the wobbulator or from the sample object, which leads to errors in measurement.

These deficiencies can be avoided if you use a superheterodyne receiver as a detector which is tuned synchronously with the wobbulator. Since the receiver can attain a sensitivity of -100 dBm without difficulty, you can work with low signal levels. Nevertheless, a measurement dynamic range of over 60 dB is possible, and the measurement receiver does not allow any false measurements due to harmonic waves and spurious emissions to arise in the signal.

A spectrum analyser can be recommended as a measurement receiver, since it can already provide all the operator functions which the sweep test rig requires. Defined adjustment of the central frequency and the sweep width is available, the amplitude scale is dB linearly calibrated, the measuring band width and the sweep speed are adjustable, and the high stability of the oscillators allows narrow-band filters to be measured as well. For these reasons, many analysers are equipped, internally or externally, with a following transmitter which transmits on the reception frequency, in order to allow additional sweep measurements.

The sole disadvantage of this measurement technique is that frequency conversion circuits can not be measured without additional

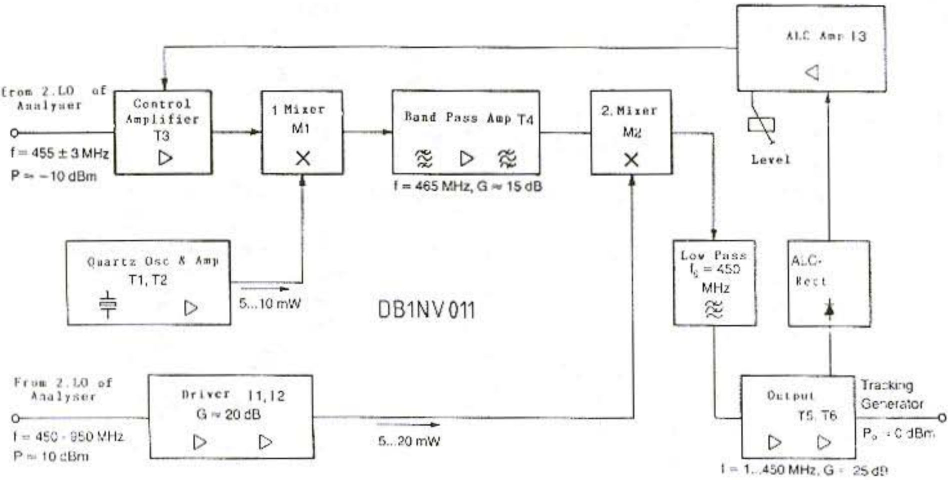

Fig.2: Block Diagram of the Tracking Generator

facilities. For this purpose, an adjustable frequency offset would also be necessary between the transmitter and the receiver. But this function is only available from the newest test rigs, e.g: spectrum analysers from Rohde and Schwarz. But the amateur can usually manage without this function.

The following section describes the basic structure of a tracking generator.

2. STRUCTURE AND USE OF A TRACKING GENERATOR

The tracking generator's job is to generate a signal which corresponds exactly to the reception frequency of the analyser. We must take into account here that for large sweep widths the first oscillator of the analyser is swept, while for small sweep widths it is the second oscillator. Thus both oscillators must be brought into the frequency processing in suitable fashion.

The solution proposed here represents the exact opposite of the frequency processing used in the analyser. Initially, a 10.7 MHz (f_z) quartz oscillator is mixed with the second oscillator (at 455 +/-2 MHz)f_{LO2} and the total frequency is amplified. The total frequency of 465 MHz corresponds to the first intermediate frequency of the analyser. This signal is mixed with the first oscillator of the analyser, f_{LO1} (from 465 to 915 MHz) and the difference is low-pass filtered and amplified, so that the generator signal corresponding to the input frequency is generated. Fig.1 shows a greatly simplified version of the spectrum analyser and the tracking generator operating together.

This circuit engineering sounds simple. But on closer observation some pitfalls appear which have to be evaded through the circuit engineering and the structure:

➡ The difference in levels between the input sensitivity of the analyser and the output power of the tracking generator amounts to about 100 dB, so careful screening and choking are an absolute must!

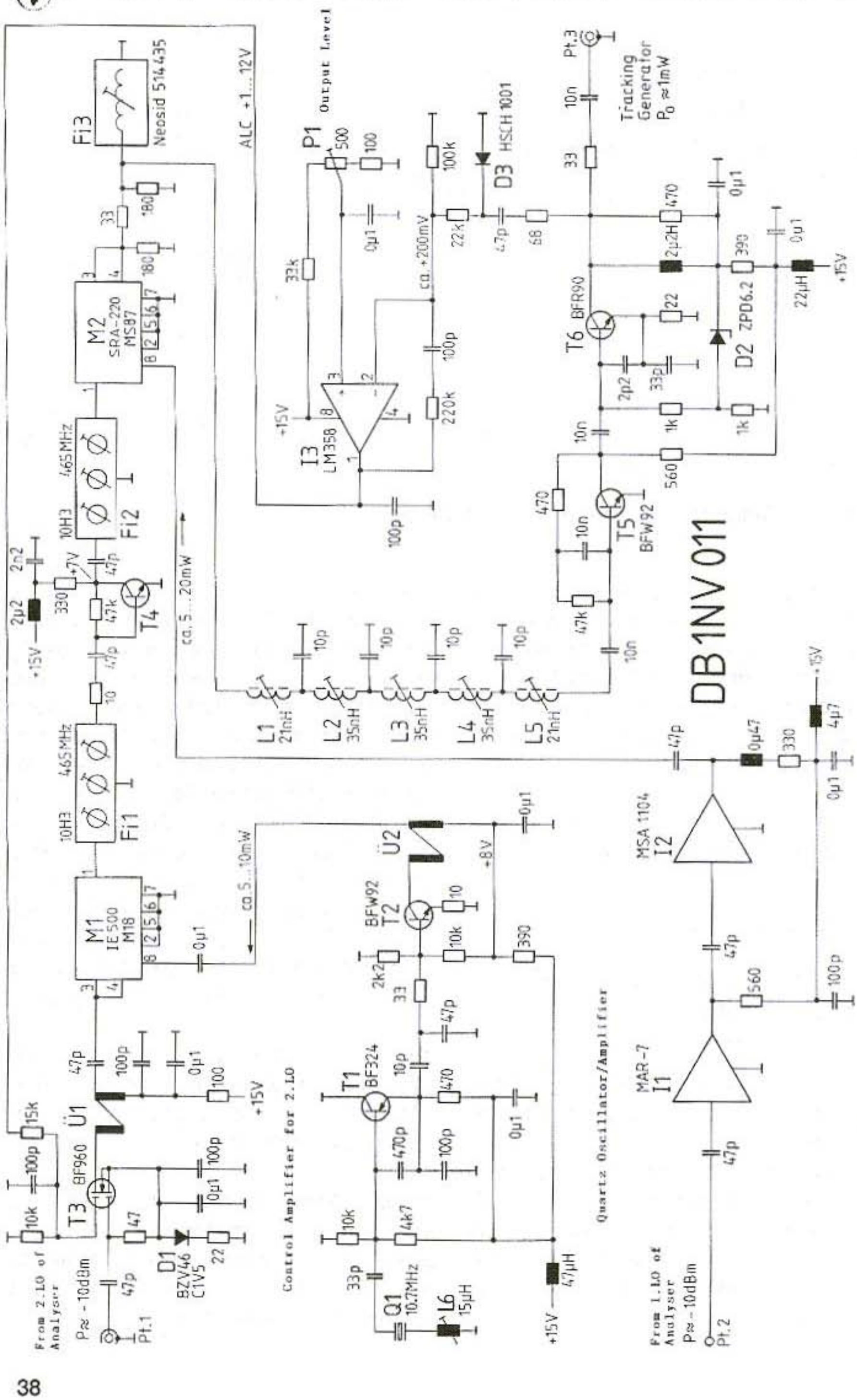

Fig.3: The full Circuit Diagram of the Tracking Generator

➡ The 10.7 MHz from the quartz oscillator can reach the intermediate frequency section of the analyser through the mixer of the tracking generator and generate a basic signal there. A separator stage for the 455 MHz signal with increased reverse damping is of assistance here.

➡ The intermediate frequency of the 465 MHz tracking generator can cut across the second mixer of the generator and the first mixer of the analyser, which is also expressed by a restriction of the dynamic range. A low pass at the generator output with a trap for 465 MHz solves this problem.

➡ Similarly, the first LO of the analyser can cut across the second mixer of the tracking generator and appear at the output. A low pass at the output can be of assistance here, too.

➡ Since the signal levels involved continuously fluctuate during the operation of the analyser, automatic volume control should also be provided to keep the input level constant at, for example, 0 dBm.

A suitably expanded block wiring diagram for the tracking generator is shown in Fig.2. This includes the ancillary stages just described, together with the most important amplification and level values. There now follows a brief description of the detailed circuit built up in Fig.2.

3. THE CIRCUIT IN DETAIL

Fig.3 shows the circuit of the tracking generator in detail. The 10.7 MHz oscillator constitutes the input point of the circuit. This is a Clapp oscillator with T1 as the active element. In order to attain a large pull-in range, the quartz is operated in series with a series oscillatory circuit (L6 and 33pF). Deviations from the average frequency of the quartz filter can thus easily be caught. The transistor, T2, a BFW92, amplifies the oscillator signal by about 5 to 10mW and operates the ring mixer, M1. At this point, any standard ring mixer, similar to an IE500, such as, for example, an Anzac MD108, or an M18 from R & K Laboratories can be used.

The signal picked up from the second oscillator of the analyser is at the intermediate frequency input of the mixer. Decoupling requires a MosFET stage in the form of a narrow-band circuit with T3. The amplification of this separator stage is close to 1 and can be adjusted using the gate 2 circuit, which is used for the volume control to be described below.

The filter at the output of the mixer, M1, allows only the total frequency from the quartz oscillator and the first oscillator to pass through. Here the same 10H3-460 helix filters are used as in the intermediate frequency section of the analyser. In order to obtain the necessary amplification in a single stage, the subsequent amplifier, T4, is fitted with the Avantek AT41485 transistor. The 10 ohm resistance in the basic circuit suppresses parasitic oscillations in the GHz range, which usually make themselves noticeable merely as too low an amplification of the stage.

An additional helix filter is provided between the amplifier and the second M2 mixer and guarantees the necessary freedom from spurious emissions for the intermediate frequency signal. The amplification of the 465 MHz intermediate frequency amplifier between the first and the second mixers is 15 dB.

The task of the second mixer is to form the differential frequency between the tracking generator intermediate frequency and the first oscillator of the analyser. To this end, the intermediate frequency of 465 MHz is fed in at the radio frequency input of the mixer and the differential frequency is fed out from the pulse frequency output. The oscillator signal from the analyser (level approximately -10 dBm) is amplified in two stages by about 20 dB before reaching the mixer, M2. In order to make the additional construction easier, two integrated high frequency amplifiers are used for the purpose, namely the MAR-7 from Mini-Circuits in the first stage and the more powerful MSA 1104 from Avantek in the second stage. The mixer, M2, is an SRA 220 from Mini-Circuits or an MS87 from Tele-Tech.

The second mixer is followed by a damping element and a low pass filter with a limiting frequency of 450 MHz. The filter is equipped with ready-made coils from Neosid, which guarantees a repeatable filter characteristic. A single helix circuit which increases the filter flank gradient is connected up at the filter input.

The output signal of the tracking generator is already available at the filter output. A two-stage broad-band amplifier (T5 and T6) raises the level to about 1mW. Because of the frequency characteristic of components and the fluctuating oscillator level of the analyser, the output level of the tracking generator is not stable enough without additional regulation. So the high frequency voltage is measured at the collector by T6 using D3, and compared with a DC voltage fed to P1 through the automatic volume control amplifier, 13. The output from I3 is controlled by the gate 2 voltage of the buffer transistor, T3.

The high frequency voltage at the collector is thus maintained constant through the control circuit with I3 and T3. This means that the high frequency output resistance of T6 in the operating range for control is almost zero. If the sample object to be energised is connected via a 50 ohm resistance, it seems to be a perfectly tuned signal source. Then since only half the collector voltage is applied to a tuned sample object, the circuit described would lead to a compromise being struck between tuning and the output power available, and the 33 ohm series resistance would be selected. The VSWR of the source is thus still better than 2. This trick can also be found more often in commercial sweep generators, the aim being to enhance the output power.

4. ASSEMBLY AND CALIBRATION

With regard to the assembly of the structural components of the spectrum analyser also, the principle is that, as far as possible, only the elements listed should be used, so as to avoid mechanical and electrical problems. In particular, the use of other filters and coils makes tuning work unavoidable. The parts list below gives the precise references of the elements in question.

4.1. Components

Semiconductors:

T1:	BF 324 (Siemens, Philips)
T2, T5:	BFW 92 (Siemens, Philips, Motorola)
T3:	BF 960 (Siemens)
T4:	AT4185 (Avantek, BFI works in Eching)
T6:	BFR 90 (Siemens, Philips, Motorola)
D1:	BZV46C1V5 (Philips)
D2:	ZPD6.2(ITT)
D3:	HSCH 1001 (Hewlett-Packard)
I1:	MAR-7 (Mini-Circuits)
I2:	MSA 1104 (Avantek)
I3:	LM358 (various manufacturers)

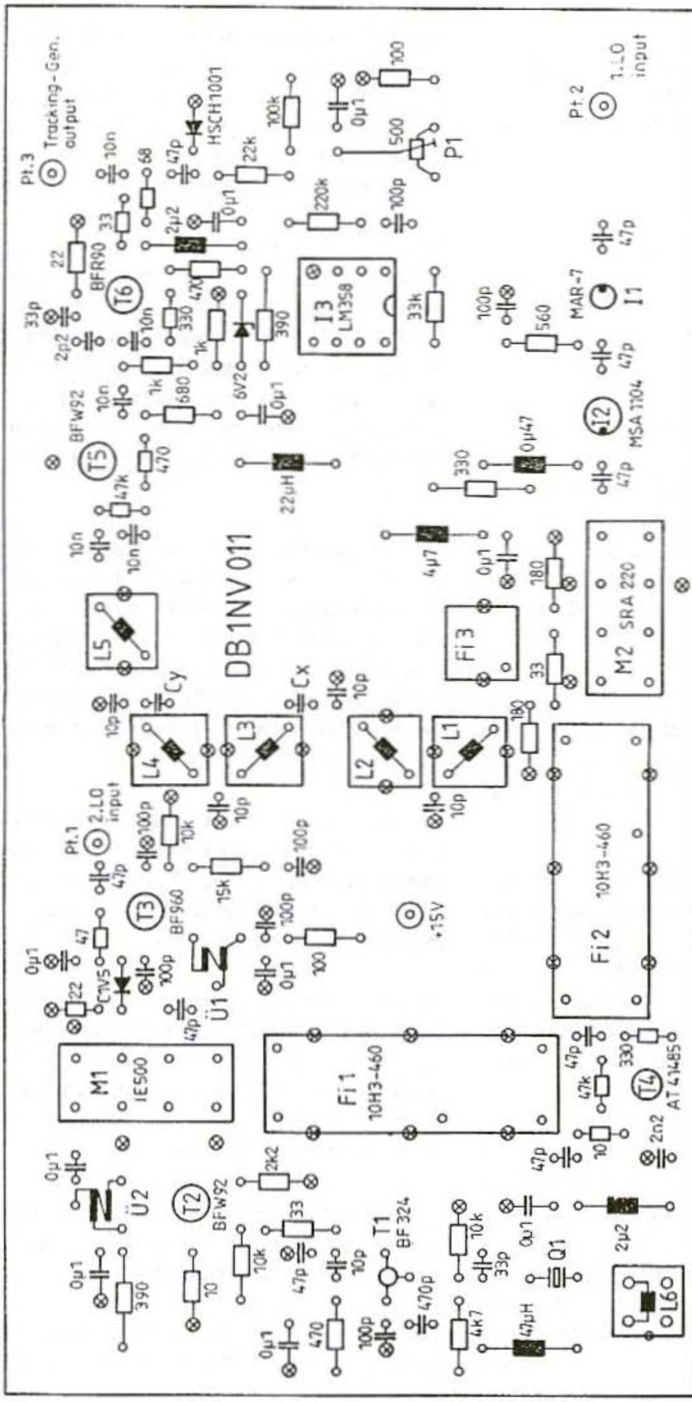

Fig.4:
Component Layout for the Tracking Genrator circuit board DB1NV011

Mixers:

M1:	IE500, M18 or other standard ring mixers up to 500 MHz
M2:	SRA220, MS87 or other ring mixers up to 1.5 GHz

Coils/transformers:

Fi1, Fi2:	10H3-460 helix filter (Tele Quarz)
Fi3:	514435 helix circuit, 464 MHz (Neosid)
L1, L5:	514831 21 nH ready-made coil (Neosid)
L2, L3, : L4	511631 35 nH ready-made coil (Neosid)
L6:	25 Wdg 0.15 CuL on 7F1S kit (Neosid)
U1:	2 x 2 Wdg 0.15 CuL on FB101-43 ferrite bead (Amidon)
U2:	2 x 4 Wdg 0.15 CuL FB101-43 on ferrite bead

As regards the passive components, attention should be paid only to small modern structural forms. Some resistances are designed for grid 5mm. HFC's ("hard-to-fit components") can be dispensed with.

With regard to the assembly and calibration, apart from a multimeter and an oscilloscope with a band width of approximately 20 MHz, a sweep generator (0 to 500 MHz) is required for the 455 to 465 MHz ZF and the low pass calibration. It is best to approach the assembly step by step, checking the individual stages as you go.

Since the DB1NV011 printed circuit board is coated on both sides for screening reasons, before the components are fitted the component bores must be drilled to give a clearance using a 3mm drill. This does not apply to the earth connections of the components, which are soldered to the top or bottom of the printed circuit board. These points are marked with a cross on the fitting plan (Fig.4). Before beginning work on the assembly, it is recommended that you read through the following paragraphs carefully. If you move too fast, you may find yourself having to desolder one or two components when you get to the calibration!

It is best to start the assembly with the quartz oscillator, the first step here being to wind the pull-in coils L6 and the broad-band transformer U2. The winding data can be found in the parts list. As regards the fitting, you merely have to pay attention to mounting T2 correctly. It is inserted into a 5mm bore in the printed circuit board, with the markings facing down.

The M1 ring mixer is not fitted initially, but instead a 47 ohm resistance is incorporated from connection 1 to earth and acts as a terminal resistance for the oscillator signal. If a test is now carried out in which the operational voltage of 15V is applied, a high frequency level of approximately 2Vss should be measured at the terminal resistance.

You should also check that the oscillator swing does not become intermittent when the core of L6 is fully rotated. The pull-in range of the oscillator can be determined using a frequency counter. It will be about 20 kHz.

Next you construct the buffer stage with T3. The dual-gate MosFET should also be fitted into a bore in the printed circuit board, only here the markings side points upwards and the source connection (thicker terminal lug) points towards the M1 mixer.

In winding the repeating coil, U1, make sure both part windings are cleanly drilled. Otherwise, the buffer stage amplification is too low.

The operation of the buffer is tested using the sweep generator at 455 MHz. The throughput amplification from the "2nd oscillator" input

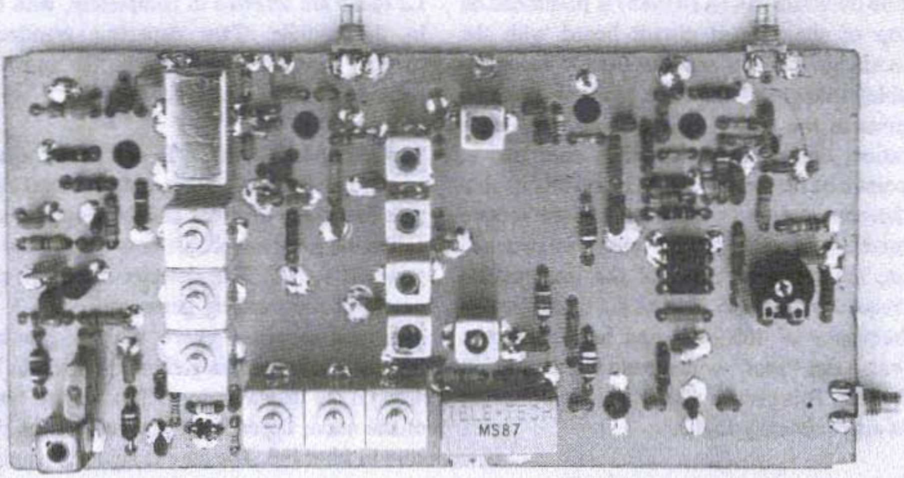

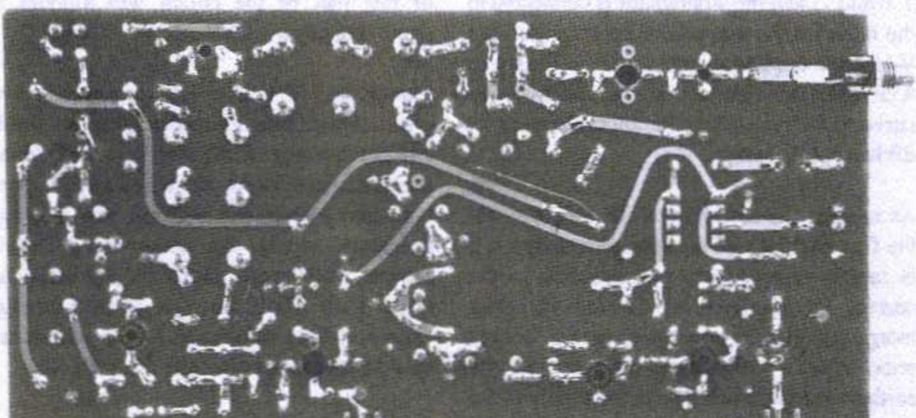

Fig.5: A specimen of the DB1NV011 Tracking Generator

to connection 3 and 4 of the M1 mixer is at approximately 1 if about 4V are applied to gate 2 of T3. It can be reduced to almost 0 if the gate-2 voltage is reduced.

Following the buffer stage, the intermediate frequency amplifier is fitted for 465 MHz. To this end, six earth bores are drilled out to approximately 1.7mm for each helix filter, and a 2.5mm bore is drilled out for T4. The helix filters are soldered to the earth lugs above and below. A sufficiently large soldering iron should be used for this. The author used a temperature-controlled 50W soldering station.

The transistor, T4 (AT41485) is positioned on top of the printed circuit board with the markings side up and the (barely recognisable) triangle of the base marking pointing towards the pull-in coil, L6. For the calibration, the sweep generator is energised at point 8 of the first mixer, M1, and the 50 ohm detector comes to connection 1 of the second mixer. When the supply voltage is switched on, the response curve of the intermediate frequency amplifier is to be set to an average frequency of 465 MHz and best symmetry, with a flat "roof" with a band width of about 5 MHz. This gives a throughput amplification of approximately 15 dB.

The mixer, M1, is then soldered on (don't forget earth through plating at connections 2, 5, 6 and 7) and the wobbulator is connected to the input for the second oscillator (point 1). 4 V is again applied to gate 2 of T3. Tuning to 455 MHz now gives you the entire sweep curve as before, only with approximately 10 dB less amplification.

As regards the assembly of the amplifier for the first oscillator of the spectrum analyser, it is merely necessary to pay attention to the correct incorporation of I1 and I2. Both integrated circuits are fitted to the bottom once suitable bores have been drilled, the earth connections being soldered tightly to the housing and bent upwards and soldered to the top of the printed circuit board. The housing mark on I1 (violet spot) points towards point 2 and the mark on I2 (button) points towards the mixer, M2. The mixer, M2, has not yet been fitted!

As regards the assembly of the low pass filter, attention should be paid to correct coil fitting. The Neosid coils used can be distinguished only by the colour of the coil body (visible in the core aperture). The 21nH coils are green, the 35nH coils yellow and the helix circuit blue. After incorporation, the brass cores from L2 to L5 are screwed in completely, with L1 in the middle. Two capacitor positions, marked on the fitting plan as Cx and Cy, remain free in the vicinity of the filter.

The amplifier transistors, T5 and T6, are again inserted into suitable bores with the markings side down. The low pass and the amplifier are calibrated using a wobbulator at connection 3, powered by M2. The detector comes to the output of the tracking generator, point 3. A low pass response curve with a limiting frequency of approximately 460 MHz can be seen on the display screen. The precise form of the curve depends on the position of the core in filter Fi3. The core is adjusted using a non-metallic tool so as to obtain a flank which drops steeply at 450 MHz. The amplification of this part of the circuit will amount to approximately 20 dB.

The mixer, M2, is inserted last, and the entire printed circuit board is soldered into a suitable tinplate housing. Fig.5 shows a fully-fitted printed circuit board which has not yet been built into a screening housing. For the high frequency supply, the author used Subvis sockets, with the operational voltage being fed from 1 to 10nF through a feed-through capacitor. Fine calibration is not undertaken until after incorporation into the analyser.

5. INCORPORATION INTO THE SPECTRUM ANALYSER AND FINAL CALIBRATION

As regards connecting the tracking generator up, the outputs for the first and second oscillators are retrofitted first. The first oscillator can be tapped from the "LO out" socket provided in the DB1NV007 assembly if the resistance divider 560/68 ohm is altered to 330/68 ohm. If you have not incorporated this

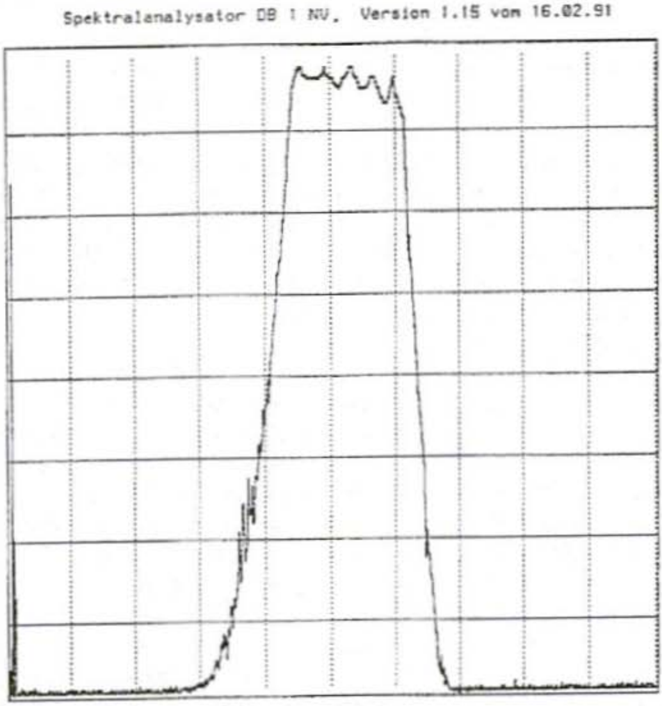

Fig.6:
Working example: a Weather Satellite Quartz filter 10.7MHz;
X = 20kHz/division
Y = 10dB/division

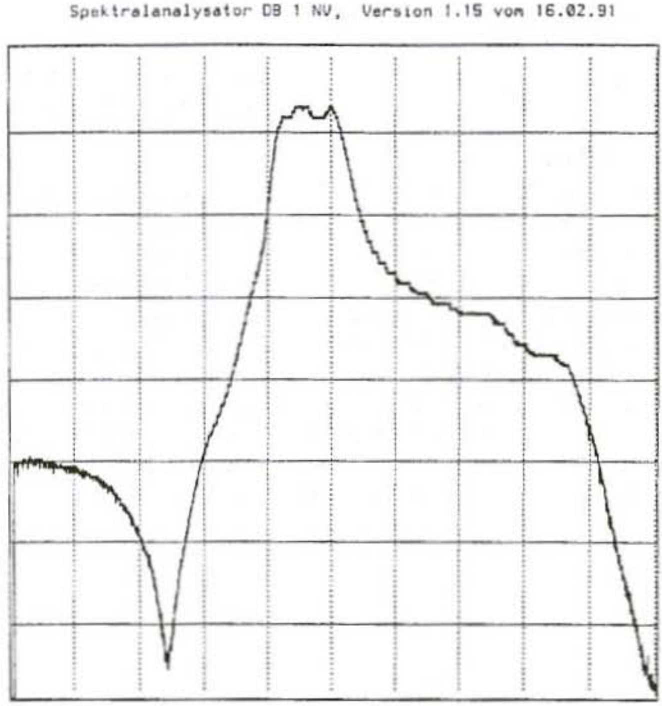

Fig.7:
Working example: a Helix filter for 435 MHz
X = 10MHz/ division
Y = 10dB/division)

output yet, the additional sockets and the two resistances can easily be housed directly at the output of T1 (BFG96).

As regards the tapping of the second oscillator in the DB1NV007 assembly, a resistance divider with 330/68 ohm is connected to the 6pF trimmer/damping element connection point, so that the decoupled oscillator level is approximately -10 dBm. If the second oscillator has already been converted into a ceramic resonator, the tap point lies at the cold end of the coupling coil, L1, which leads to the damping element.

As already mentioned, the output level of the tracking generator is about 100 dB above the input sensitivity of the analyser, which makes extreme demands on the reciprocal screening for direct incorporation. The author himself was unable to obtain complete decoupling using double-screened cables, and needed the assistance of a switch, which switched the tracking generator on only when it was needed.

For test commissioning, the cable connections are manufactured and the potentiometer, P1, is set on the left-hand stop. An oscilloscope is connected to pin-2 of the control amplifier, I3, (through a 10:1 probe). The output of the tracking generator (point 3) is terminated in 50 ohms and the spectrum analyser is to be set to the 200 kHz band width and the 0 to 500 MHz display width. A right-angled line with indentations and a more or less flat top appears on the screen. P1 is now turned to the right until the top becomes flat and only the indentation at the frequency "0" remains (the zero mark on the analyser screen).

The tracking generator output is now connected to the analyser input and the first oscillator is disconnected. The level now shown on the screen is the remainder of the 465 MHz intermediate frequency of the tracking generator, which passes through the second mixer, the low pass filter and the output amplifier, and thus arrives in the analyser. This signal can be brought to a minimum by calibrating the 465 MHz trap, Fi3.

The first oscillator should then be reconnected and an average frequency of 100 MHz should be applied to the analyser, with a display width of 50 kHz/cm. and an intermediate frequency band width of 1 kHz. Use the pull-in coil, L6, to trim the analyser display to a maximum. If this does not succeed, the frequency displacement between the quartz filter of the analyser and the quartz, Q1, is too great, and Q1 should be exchanged for something more suitable. You can usually find something suitable in stripped-down quartz filters.

Once this calibration has been successfully completed, the final assembly can be carried out.

Finally, Fig's.6 and 7 show two filter response curves recorded using the tracking generator. In Fig.6, the well-known QF10.7-30 quartz filter for weather satellite receivers was measured at a display width of 20 kHz/division and a level scale of 10 dB/division. As can be seen, the filter tuning was not quite right. Fig.7 shows the behaviour of a three-circuit helix filter for 435 MHz, with a 10 MHz/division display width and a level scale of 10 dB/division.

Walter Zwickel OE2TZL

A Marker Generator for 10MHz and 1MHz Markers

Marker generators are still used for all sorts of purposes, even today, in the age of the low-priced frequency counter. For spectrum analysers or sweep signal generators, for example, or to be able to check the accuracy of the frequency in receivers without electrical intervention.

The present article describes a simple circuit, which does not need costly calibration, and yet produces thoroughly usable data: 10-MHz markers between -40 and -60 dBm in a range between 10 and 900 MHz, 1 MHz markers between -55 and -65 dBm in a range between 1 and 300 MHz. Naturally, markers can still be indicated up to significantly higher frequencies, but the amplitudes decrease sharply.

1. FUNCTIONAL DESCRIPTION

A 74LS00 functions in a known manner as a quartz oscillator at 10 MHz (Fig.1). Naturally, the relatively high quartz stress through the simple oscillator circuit brings with it a certain ageing of the quartz. However, in this application the highest levels of frequency constancy are not required. But, on the other hand, a high-constancy 10 MHz signal with a TTL level can easily be fed in to take the place of the oscillator.

In the later 74LS690, the frequency is divided by 10, so as to generate markers at 1 MHz intervals as well. The two-way switch selects one of the two markers using the open collector technique.

The later NAND gate in the advanced low-power Schottky technology, a 74ALS00, has a very short gate transit time, and aims to produce a delay in the region of a few

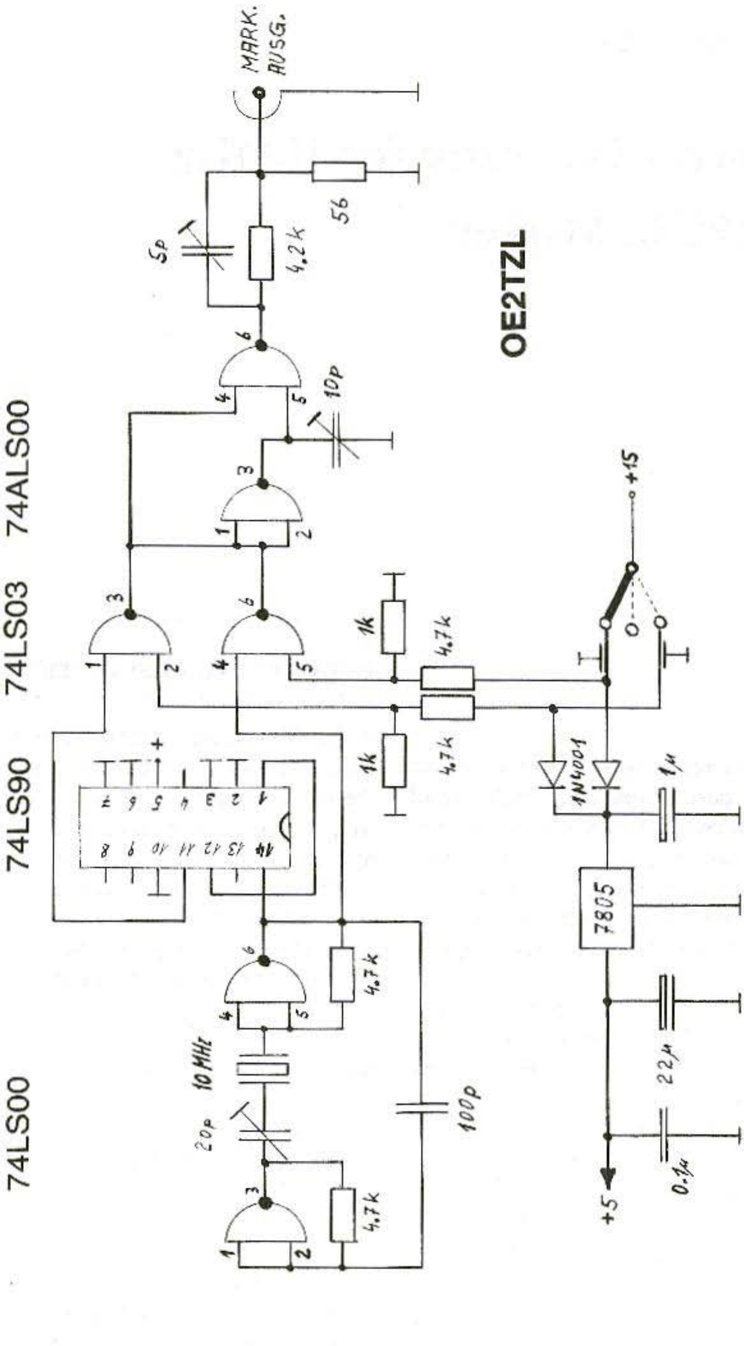

Fig.1: Circuit Diagram of the Frequency Marker Generator

nanoseconds, which can be adjusted, within limits, using the 10pF trimmer. This type of delay has led to better results than using 2 or 3 gates.

In the last gate, the delayed signal and the direct signal are combined to form a very short spike pulse. The skirt gradient decides the harmonic wave spectrum!

To obtain the highest possible limiting frequency, a 74ALS00 must be used, or, if applicable, even a 74F00.

Behind the last NAND gate, a compensated voltage divider provides an initial voltage, halfway independent of the frequency, which is tuned to 50 ohms. A 7805 voltage controller provides the four TTL integrated circuits.

2. ASSEMBLY

To keep the cost low, the development of a circuit board was dispensed with, since things move just as fast with a single-sided coated epoxy board.

Here the coated side is used as a continuous earth surface, since we are always dealing with frequencies in the UHF range here. The small number of connections are made on the underside, using thin wire. No mountings should be used.

Make sure the lead cable is as short as possible, especially in the section around the 74ALS00.

The obvious idea of using the remaining gates of the 74ALS00 for the oscillator, in order to save the need for an integrated circuit, can not be recommended, for two reasons. Firstly, using this type of equipment involves a considerable increase in the quartz stress, andsecondly connections within the integrated circuit lead to a sharp drop in the upper frequency limit.

3. CALIBRATION

First, the exact quartz frequency of 10 MHz must be set on the 20pF trimmer, either by monitoring the zero beat frequency on the short-wave receiver using one of the known normal frequency transmitters such as WWV, or by means of the frequency counter, which is connected to pin-6 of the 74LS00 through a small coupling capacity of approximately 10pF.

With a spectrum analyser, the two trimmers can be calibrated alternatively at the start to an amplitude spectrum of 10 MHz markers as constant as possible. If no spectrum analyser is available, the following trimmer setting is also adequate: 10pF trimmer to centre, 5pF trimmer almost turned off.

The complete little unit comes in a metal housing, with two 1nF feedthrough capacitors for the two-way switch. This is externally mounted, as it feeds in only DC. Any sockets, such as SMA, SMC or BNC, can be used for the HF output.

Walter Zwickel OE2TZL

Expanding the DB1NV Spectrum Analyser to 2GHz

Many people building on the very well thought-out DB1NV analyser have certainly already bemoaned the measurement gap in the range between 500 and 1,000 MHz. In order to help get round this, a 2 x VCO has been developed, which is capable of providing a power level of almost 10 mW in the 1000 - 1500 MHz range. Provided the first mixer is good enough, the 1500 - 2000 MHz range can also be covered using the image frequency.

1. CIRCUIT DESCRIPTION

Only the standard components familiar to the average amateur were available to develop the circuit. So it was clear from the start that trade-offs would have to be taken into account with regard to the technical data of the VCO. But these disadvantages in no way resulted in unstable tuning behaviour, still less in reverse tuning. Certain variations over the frequency range, which affected only the amplitude constancy, could be accepted, as long as it was ensured that the diodes in the ring mixer were controlled in a sufficiently advanced manner.

Countless experimental expansions were undertaken in the search for the most suitable tuning diodes and the most favourable oscillator transistor (T2). Surprisingly, a standard UHF type, namely the BF979, gave the best results, provided it was subjected only to a weak load initially. This could be achieved using the highly-amplified BFG 96 (Fig.1).

This explains the unusual decoupling at the oscillator transistor - direct decoupling at the emitter would require minute capacities and in addition impair the amplitude response.

The oscillator booster amplifier (T3) was taken over in its entirety from the original construction instructions. It should be noticed here that the BFG96 DC amplification pro-

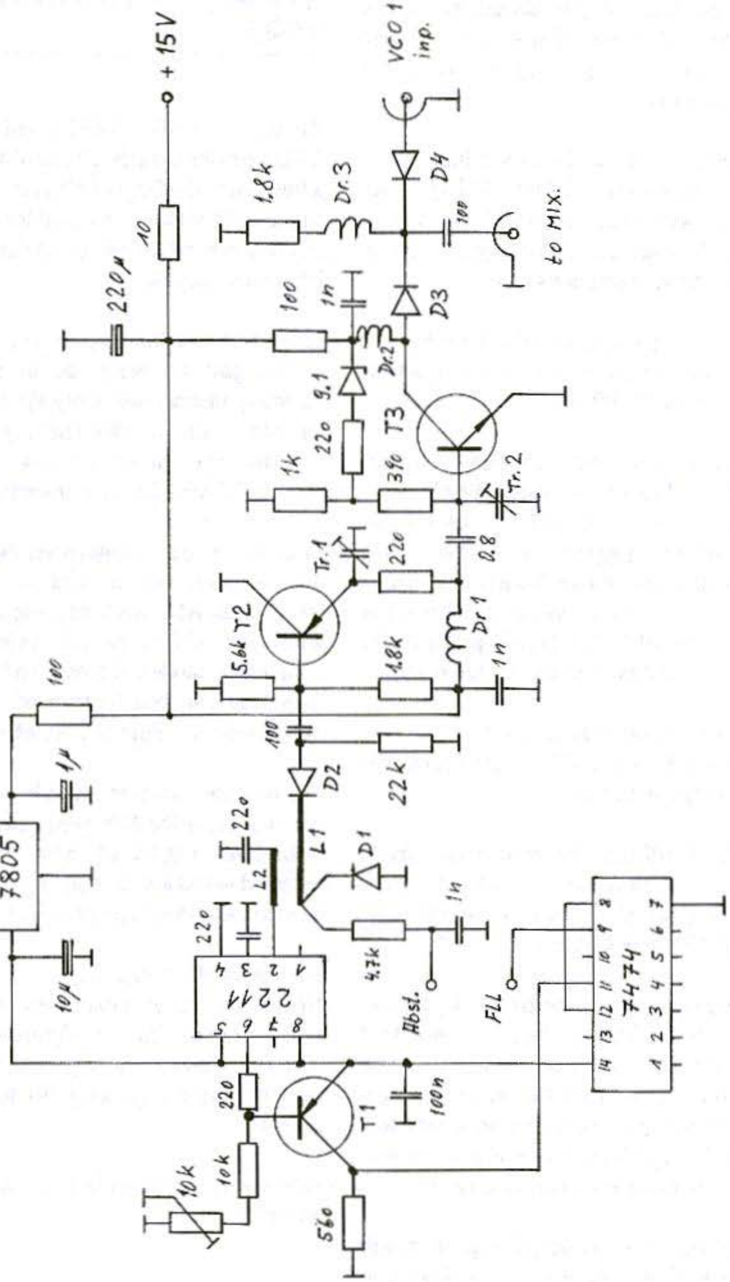

Fig.1: A second VCO which extends the frequency range of the DB1NV Spectrum Analyser to 2 GHz

duces a high level of diffusion. For this reason, the basic divider should be dimensioned in such a way that a collector zero signal current of approximately 30 mA is flowing (A mode).

The chokes proved to be very critical. They were developed on a 2.5mm drill and subsequently somewhat stretched, so that a winding interval correspondingly approximately to the wire thickness arose.

L1 acts as a (lambda)/2 circuit, which is tuned on both sides. This is the only way to attain the required stroke of 500 MHz.

Initial fears of too much phase jitter with this circuit proved to be unfounded. Freely oscillating, it lies at about 50 kHz - only if the tuning voltage supplied is hum-free and low-resistance, of course. When connected to the FLL, this VCO is even somewhat better than the original VCO. This is probably the result of the relatively narrow tuning width.

The SDA2211 was used to divide by 64, as it operates reliably up to 1.7 GHz and consumes less current than the 4211.

The FLL and PLL no longer operate reliably at a maximum output frequency of 23.5 MHz. For this reason, a 7474 was mounted inside the actual VCO housing to divide by 2.

The compensating resistances in the current supply are no luxury. Even in industrial circuits, the same sin is committed here time and again. Because of the extremely low dynamic internal resistance of good tantalum electrolytic capacitors, these are often destroyed when the apparatus is switched on.

Damaged tantalum electrolytic capacitors will be a thing of the past if you take this tip to heart.

2. ASSEMBLY INSTRUCTIONS FOR VCO 2

An additional DB1NV007 board proved useful in assembly, making it possible to build up a frequency divider, an ECL converter, a 7805 and a 7474 without any problem. The board can be sawn off on the left of the first row of integrated circuits.

The VCO 2 is built up on the fully-coated surface just as easily as in the original assembly instructions. Only the layout of the modules will be different, as would be expected. Fig.2 provides a view of the layout of the VCO with the booster amplifier.

Make the module connections the very shortest possible, on account of the higher frequencies. After soldering, there must be no wires left visible in the vicinity of the capacitance diodes, the base and the emitter. Only thus can you be sure of attaining the upper frequency limit of 1500 MHz.

The proposed structure must be adhered to in the vicinity of the PIN diode switch as well. Noticeable lengths of wire here will be reflected in too low an output power, and also in wide variations in power over the range.

The decoupling capacitor can be a small 100pF capacitor with extremely short wires or a chip format. Use an ohmmeter to check whether a connection is present through this capacitor before hooking up to the mixer assembly.

This measure can save the expensive ring mixer!

2.1. Parts list

Semiconductors:

T1:	BF 970
T2:	BF 979
T3:	BFG 96
D1:	BB 405
D2:	BB 405
D3:	BA 379
D4:	BA 379

Inductors:

L1:	10 mm. CuAg; 1 mm. dia., 4 mm. over earth
L2:	5 mm. connection wire of 220-pF capacitor 4 mm. from L1
Dr 1:	2.5 Wdg. on 2.5-mm. pin; 0.4 mm. Cu alloy, loosely wound
Dr 2:	3 Wdg. on 2.5-mm. pin; 0.4 mm. Cu alloy, loosely wound
Dr 3:	5 Wdg. on 2.5-mm. pin; 0.4 mm. Cu alloy, closely wound

Capacitors:

4 1 nF/50 V discs, not wired up
All other capacitors: ceramic RM 2.5
Electrolytic capacitors: Tantalum 16 or 25 V

Trimmers:

Tr1:	5 pF Teflon (SKY)
Tr2:	5 pF Teflon (SKY)

Resistors:

Both 100 ohm in the 15-V supply: 1/3 W
All others: 1/8 or 1/10 W

Other Components:

1	DB 1 NV 007 board
1	tinplate housing, 54 x 148 x 30mm (or shorter)
3	SMA, SMC coaxial sockets
2	1nF feed-through capacitors
1	relay

3. CALIBRATION

The VCO 2 can easily be calibrating using the analyser already constructed in the 1000 - 1500 MHz range. For this purpose, a damping element of at least 10 dB, suitable for this range, should be inserted. The tuning voltage is then generated by an external 30 volt power source via a 4.7k potentiometer. 1500 MHz should be reached at 27 volts maximum, otherwise L1 should be shortened by 1mm, or the structure should be checked for over-long connecting wires!

Trimmer 1 is calibrated at the most constant amplitude possible, and trimmer 2 at the maximum output power. Trimmer 1 will probably have to be almost turned off. This is normal. The only way to improve the adjustment would be by using an expensive microwave trimmer.

Should the output power vary by more than 5 dB over the range between 1000 and 1500 MHz, choke 1 can be given half a winding more or less as an experiment, depending on whether the smaller power level is at the top or the bottom end of the band. In the sample apparatus, it was possible to reduce the oscillation to 3 dB (5 - 10 mW). If these results are achieved, the DB1NV assembly can be modified, and the new VCO can be incorporated into the analyser. This makes available a measuring apparatus which can be used up to 2 GHz without any gaps.

4. MODIFICATIONS TO THE DB1NV007 MODULE

In the original VCO module, the line from the ECL level converter to pin-1 of the 74HC00 has to be interrupted and connected through a

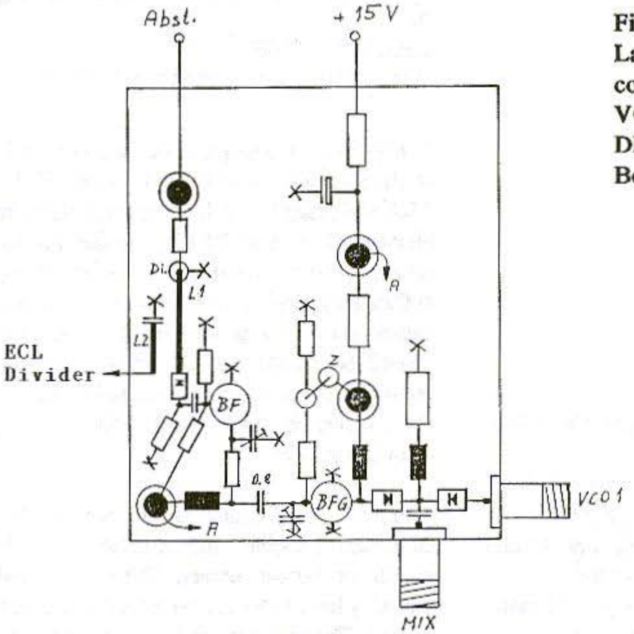

Fig.2: Layout of the critical components of the second VCO mounted on a DB1NV007 Printed Circuit Board

small relay. Thus the divider output from VCO1 or VCO2 can be fed to the 74HC00 pin-1 as desired, depending on the frequency range in the circuit. The line from VCO 2 to the relay input must naturally take the form of a coaxial cable. The control voltage for the relay can be drawn directly from the control voltage of VCO 1.

In VCO 1, the decoupling capacitor must be removed and replaced by a thick wire bridge so that the PIN diode switch can operate. In addition, the VCO 1 must be insulated from the normal +15 volt supply and must have its own operating voltage supplied through a feed-through capacitor.

In the specimen apparatus, a 4-step range selector switch was mounted on the front plate. This switch must switch only the operating voltage of +15 volts for whichever VCO is required. Four voltage dividers are also switched through this switch so that the LCD module can have a display with the correct frequency.

5. LITERATURE

Dr. Ing. J.Jirmann: A Spectrum Analyser for Amateurs:
Part-1: Design Considerations VHF Communications 3/87, pp. 154 - 166.
Part-2: Circuits, VHF Communications, 4/87, pp. 232 - 242.
Part-3: Construction with Circuit Boards, VHF Communications 2/89, pp. 108 -119.
Part-3a: Construction and PCBs, VHF Communications 3/89, pp. 163 - 171.
Part-3b: Circuit Options and Ancillary Equip't, VHF Communications 1/90, pp. 5 - 9.
Practical Tips for the Amateur, VHF Communications 3/90, pp. 130 - 138.
Enhancements to the Spectrum Analyser, VHF Communications 2/91, pp. 80 - 88.
Digital Image-Store for the Spectrum Analyser: Part-1, VHF Communications 3/91, pp. 130 -146.
Digital Image-Store for the Spectrum Analyser: Part-2, VHF Communications 4/91, pp. 229 - 233.

Dr. Volker Grassmann DF5AI

Incoherent Scatter: Principles and Applications

Classical electrodynamics teaches that a free charged particle is accelerated in an electromagnetic wave field and excited to radiation, the emission (in the non?relativistic case) being of the same frequency but in other spatial directions with respect to the incident wave. This process can also be interpreted as scattering of the incident wave (Thomson scattering), with a backscattered cross-section allocated to the charged particle as scatter body. The "Thomson scattering cross-section" for electrons is of the order of magnitude of 10^{-24} cm^2.

In 1958, Gordon proposed that scatter experiments, using radar, be attempted on the electrons present in the ionosphere (2), the technical feasibility being demonstrated by Bowles in the same year (1).

In this article, the basic physical principles of incoherent scatter are clarified, using the example of the European EISCAT installation. In contrast to ionospheric echo sounding, the VHF and UHF incoherent scatter radar units make measurements possible in all height ranges of the ionosphere and supply numerous parameters for descriptions of the temporal and spatial changes in the ionosphere.

1. THE EISCAT INSTALLATIONS IN NORTHERN SCANDINAVIA

There are seven incoherent scatter installations in the world altogether. Two particularly powerful radar systems are operated north of the Arctic Circle by the European Incoherent Scatter Association (EISCAT). The organisation represents a joint scientific effort by several countries: Finland, Norway, Sweden, Great Britain, France and Germany.

The EISCAT system consists of a transmitter/ receiver installation in Tromso, in Norway,

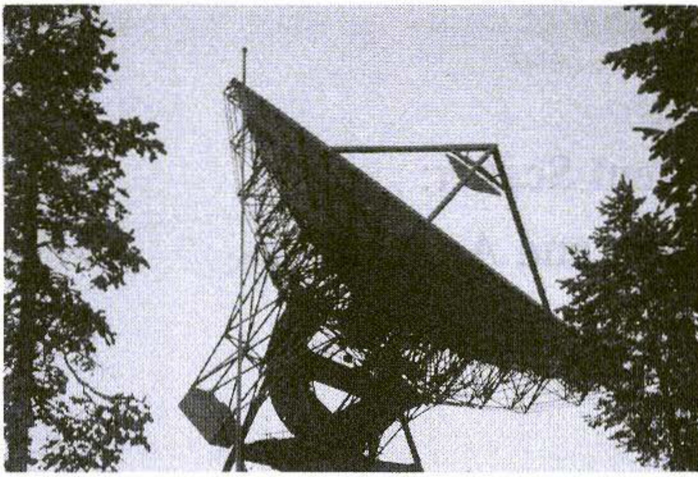

Fig.1: The 32M Parabolic Mirror with Cassegrain Exciter at the EISCAT receiver Station in Sondankylä, Finland. Systems of similar construction are located in Tromsö, Norway and in Kiruna, Sweden. An aerial gain of 48 dB is achieved at the operating frequencies around 931 MHz. The width of the main lobe is 0.6°. (Photograph DF5AI).

and two receiver stations, one in Kiruna (Sweden) and one in Sodankylae (Finland). The transmitter's peak power is 1.7 megawatts at 931 MHz. Each of the three sites has a 32M. dish aerial (Fig.1). The installation in Kiruna is not unknown to radio amateurs, for the dish aerial there has already been used for EME purposes (6).

The 224 MHz VHF installation is also in Tromso. At the moment, the transmitter is being used with a peak power of 1.5 megawatts, and the final transmission power will be 4 megawatts. A dish cylinder aerial measuring 120M x 40M is available as transmitter and receiver aerial. The table below shows the most important system parameters for both installations.

The interest in the observation stations in the far North stems from the peculiarities of the polar ionosphere. The lines of the earth's magnetic field traverse the ionosphere at much steeper angles in Northern latitudes than, for example, in equatorial latitudes. Thus these field lines penetrate more deeply into the magnetosphere, which leads to numerous phenomena which are rarely or never met with in equatorial latitudes.

It may be worth mentioning that the heating installation of the Max Planck Institute for Aeronomy is also being operated in Tromso. Twelve powerful short-wave transmitters (each with a continuous power of 120 kW) bring about the active modification of the ionospheric plasma.

Some of the effects triggered by this can also be observed by the EISCAT installation. A further incoherent scatter installation is at present being planned for Spitzbergen (Polar Cap Radar).

EISCAT Parameter	UHF Radar	VHF Radar
Locations: (TR)	69° 35' N, 19° 13' E	69° 35' N, 19° 13' R
(KI)	67° 51' N, 20° 26' E	
(SO)	67° 22' N, 26° 38' E	
Average Frequency:	931.5 MHz	224.0 MHz
Bandwidth:	8 MHz	3 MHz
Pulse Power	1.7 MW	1.5 MW
Average Power:	280 kW	140 kW
Pulse Duration:	1 us - 10 ms	1us - 1ms
Minimum Pulse Interval:	1ms	1ms
Aerials:	Parabolic Mirror	Parabolic Cylinder
	32 M Diameter	40 M x 120 M
Exciter:	Cassegrain	128 Elements
Gain:	48.1 dB	43.1 dB
Polarisation: (TR)	Circular	Circular, Linear
(KI, SO)	Any	
System Temperature: (TR)	90 - 110 K	250 - 350 K
(KI, SO)	30 - 35 K	

TR = Tromsö, KI = Kiruna, SO = Sodankylä

Table: Operating Parameters of EISCAT Radar from (4, 5)

2. DESCRIPTION OF SCATTER-ECHOS

In the scatter volume of the radar aerials, the contributions from the partial waves scattered into the individual electrons are superimposed on one another without any outstanding phase relationship existing. The incoherent superimposition gave the scatter method its name.

The scatter echo recorded by the receiver is extremely weak, for even the large numbers of electrons "lit up" in the aerial lobe lead, in all, only to a small total cross-section. We imagine that the ionosphere should in general be considered as transparent at frequencies of a few hundred MHz. The difference from one hundred per cent transparency is something worth assessing, using this measurement method.

The scatter volume lit up by an ionosphere radar (circular aerial aperture at 1 degree x 1 degree, 50us. transmission pulse) in the F region (height 300 km., electron density 10^{12} m^{-3}) leads to a total scatter cross-section of approximately 0.2 cm^2.

These areas, several hundred kilometres apart, can trigger no measurement signal from a single radar pulse, so that data integration is essential. For the positively charged ions, the scatter cross-section is smaller by the factor $(m_i/m_e)^2$ (m being the individual particle mass), and so the ionic echo components are completely disregarded.

It is possible to imagine a fictitious electron distribution in which the partial waves would always superimpose to zero. In the same way, it is possible to imagine a structured distribution which favours constructive interference.

On the basis of these concepts, it can be pointed out that not only is the microscopic scatter process of importance but the macroscopic organisation of the scattering medium also plays an important part.

In reality, the electron distribution is irregular and fluctuating. This condition can be simulated mathematically by a superimposition of many short-wave and long-wave processes.

A radar installation is not in a position to do more than sense irregularities, the wavelength of which corresponds to half the radar wavelength. For example, a 2M amateur station is dependent on irregularities with a length of approximately 1M. during an Aurora backscatter, whilst correspondingly smaller structures are responsible for 70cm Aurora contacts.

This relationship applies irrespective of the primary scatter process (the Aurora backscatter events used by radio amateurs are, of course, not connected with the scatter method described here).

The irregularities in electron density are, to a decisive extent, controlled by the positive ions, which have a larger mass (and thus are better carriers). In this way, a signature for the ions in the electron density distribution is obtained. Although the incoherent backscatter is carried exclusively by the electrons, we obtain valuable data on the ions in the ionosphere for this reason.

In a similar way, and to a lesser degree, we also obtain information on the neutral particles (at the heights observed, indeed, only about one-thousandth of the atmospheric particles are ionised, the neutral gas component being the numerically dominant fraction even in the ionosphere).

3. BACKSCATTER SPECTRA

Fig.2 shows a print-out from the data monitor, which shows the instantaneous measurement results from a real experiment. The measurements were carried out using the EISCAT UHF system (3). The diagram shows the scatter echoes obtained in Finland from the Norwegian transmitter. The small partial image shows the typical double hump form of the scatter spectra.

In a real scatter experiment, we are interested in the total backscattered yield (on the basis of which is determined the electron density in the scatter volume), but predominantly in the frequency distribution of the scatter spectra (each of the electrons in motion triggers a Doppler shift, and in total these bring about a continuous total spectrum). The electron and ion temperatures (in the polar ionosphere up to several thousand K) can be derived, among other things, from the form of the scatter spectrum, but conductivity values, the number of collisions and the types of ions involved can also be determined.

The drift speed of the ionospheric plasma (up to several thousands of metres/second in the polar ionosphere) can be determined from the Doppler shift of the total spectrum. The tri?static UHF system here supplies three Doppler measurements different from one another, from which the three coordinates of the speed vector can be calculated.

With knowledge of the local field vector of the earth's magnetism, the strength and direction of the electrostatic field in the ionosphere (typical value in the polar ionosphere: 100 mV/m.) can be determined from the speed components vertical to the magnetic field ($\underline{E} \times \underline{B}$ -drift).

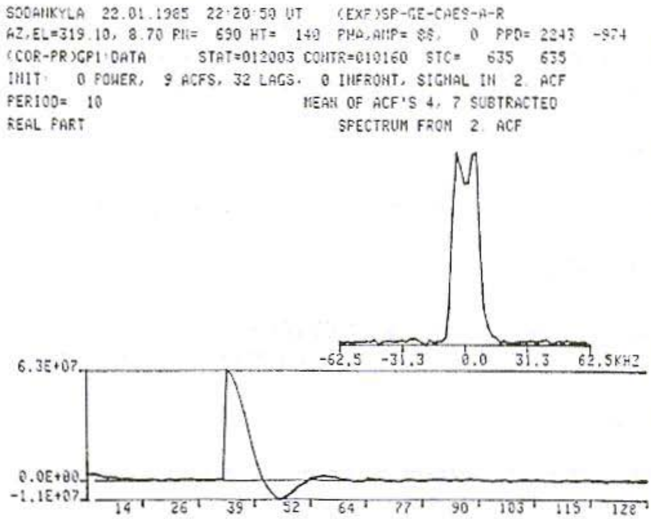

Fig.2:
EISCAT recording dated 22/01/85, Sodankylä (3). The backscatter echo originates at a height of 140 kmand is 690 km away. The lower section shows the real component of the auto correlation function, averaged over 10 secs, following a first release of noise between the lags 34 - 64. The spectrum arose from a Fourier Transformation of the complex function.

4. APPLICATIONS

Incoherent scatter radar installations make possible research into short term and long term, small scale and large scale changes in the ionosphere.

The individual measurements attain temporal resolutions in the range between tenths of a minute and minutes, but with the assistance of the data collected in previous years annual oscillations or variations, which are connected with the sunspot cycle, can also be brought out.

The spatial resolution can be a few hundred metres in the vertical or, under the influence of the earth's rotation and the position of the sun which alters with it, can indicate the large-scale horizontal structure of the ionosphere.

The incoherent scatter radar installations installed in the polar latitudes can also provide hints on the magnetospheric processes which take place many thousand kilometres above the ionosphere.

The lines of the earth's magnetic field represent equivalent potential lines, which thicken as they approach the earth from the direction of the magnetosphere. Electrical potential differences triggered in the magnetosphere are in this way reflected in the polar ionosphere under amplification.

Since the magnetospheric processes are connected with the flow of particles from the sun, ionospheric processes can also be studied in relation to the solar wind or to the sector structure of the interplanetary magnetic field. In research of this latter kind, the incoherent scatter data are combined, for example, with the results of the observations from satellite-aided experiments.

5. LITERATURE REFERENCES

(1) Bowles, K.L.:
Observation of vertical-incidence scatter from the ionosphere at 41 Mc/sec.
Phys. Rev. Lett., vol. 1, no. 12, 1958, pp. 454-455

(2) W.E. Gordon:
Incoherent scattering of radio waves by free electrons with applications to space exploration by radar.
Proc. I.R.E., vol. 46, 1958,
pp. 1824 - 1829

(3) V. Grassmann:
Incoherent backscattering of radio waves through a plasma, with consideration being given to particle collisions
Max Planck Report
MPAE-W-100-88-07, 1988

(4) J. Roettger et al.:
EISCAT annual report, 1988 Kiruna, Sweden ISSN 03492710

(5) EISCAT (information brochure)

(6) The SK2GJ Story
Dubus, no. 1, 1981, pp. 51 - 53


practical Wireless
Britains best selling amateur radio magazine
★ Practical Home-brew Projects ★
★ Regular Antenna Designs ★
★ Amateur TV & Packet Radio ★
★ News & Views ★
★ CB High & Low ★
★ Reviews ★
Published 2nd Thursday each month.
Subscriptions, £19 - UK, £21 - Europe, £22 - Rest of World.
Sample issues available for 2 IRCs or 6 UK 1st Class Stamps.
PW Publishing Ltd., Circulation Dept., Enefco House, The Quay, Poole, Dorset BH15 1PP. Tel (0202) 678558.
practical Wireless

MATERIAL PRICE LIST OF EQUIPMENT

described in VHF COMMUNICATIONS

DJ8ES	**FM ATV Receiver for the 23cm Band**		**Art.No.**	**Ed. 1/1991**
Converter				
PCB	DJ8ES 001	double-sided	6347	DM 22.00
Components	DJ8ES 001		6348	DM 179.00
Kit	DJ8ES 001	complete	6349	DM 194.00
Digital Frequency Indicator				
PCB	DJ8ES 002	double-sided	6350	DM 19.80
Components	DJ8ES 002		6351	DM 94.00
Kit	DJ8ES 002	complete	6352	DM 110.00
IF Amplifier				
PCB	DJ8ES 003	double-sided	6353	DM 15.00
Components	DJ8ES 003		6354	DM 105.00
Kit	DJ8ES 003	complete	6355	DM 115.00
Demodulator				
PCB	DJ8ES 004	double-sided	6356	DM 19.00
Components	DJ8ES 004		6357	DM 136.00
Kit	DJ8ES 004	complete	6362	DM 150.00

DBINV	**Digital Storage for the Spectrum Analyser**	**Art.No.**	**Ed. 3/1991**
PCB	DB1NV EXper.1 (ed...)	6475	DM 29.90
PCB	DB1NV EXper.11 (solder spots 2.3 x 1mm)	6476	DM 29.90
PCB	DB1NV 010	6477	DM 44.00
Special	DB1NV 010, incl. programmed EPROM	6478	DM 276.00
Components:	DB1NV 010, EPROM only	10080	DM 44.00

DD2EK	**Modifications of the FM-ATV TX DD2EK 002**	**Art.No.**	**Ed. 3/1991**
PCB	DD2EK 002	6150	DM 28.00
Kit	DD2EK 002 without crystal but with MSA1104	6152/2	DM 145.00
Crystal	DD2EK 002 please give specified frequency	6153	DM 46.00

Post and packing minimum charges DM 14.00

The above items are all supplied by, and obtained from, UKW-Berichte in Germany.

To obtain supplies please contact your country representative for details of local prices and availability. Alternatively, you may order direct from UKW-Berichte or via KM Publications, whose addresses may be found on the inside front cover of this magazine.

Plastic Binders for VHF COMMUNICATIONS

- Attractive plastic covered in VHF blue
- Accepts up to 12 editions (three volumes)
- Allows any required copy to be found easily
- Keeps the XYL happy and contented
- Will be sent anywhere in the world for DM8.00 + post and packing

Please order your binder via the national representative or directly from UKW-BERICHTE, Terry Bittan OHG (see below)

The elder editions of VHF COMMUNICATIONS are still obtainable for reduced prices from the publishers of UKW-Berichte.

Subscription	Volume	Individual copy
VHF COMMUNICATIONS 1992	each DM38.00	each DM10.00
VHF COMMUNICATIONS 1991	each DM35.00	each DM10.00
VHF COMMUNICATIONS 1990	each DM27.00	each DM 7.50
VHF COMMUNICATIONS 1988 to 1989	each DM25.00	each DM 7.50
VHF COMMUNICATIONS 1986 to 1987	each DM24.00	each DM 7.00
VHF COMMUNICATIONS 1985	each DM20.00	each DM 6.00
VHF COMMUNICATIONS 1980 to 1984	each DM16.00	each DM 4.50

(Edition 3/1982 no longer available)

Individual copies out of elder, incomplete volumes, as long as stock lasts:

1, 2, 4/1972 * 2, 4/1973 * 1, 3/1974 * 1, 2, 3, 4/1975	each DM 2.00
3, 4/1976 * 1, 4/1977 * 1, 2/1978 * 1, 2, 3/1979	each DM 2.00
Plastic binder for 3 volumes	each DM 8.00
Post and packing minimum charges	DM 14.00

Tel: 09133-47-0 * Telefax 09133-4747 * Postgiro Nürnburg 30455-858 code 760 100 85